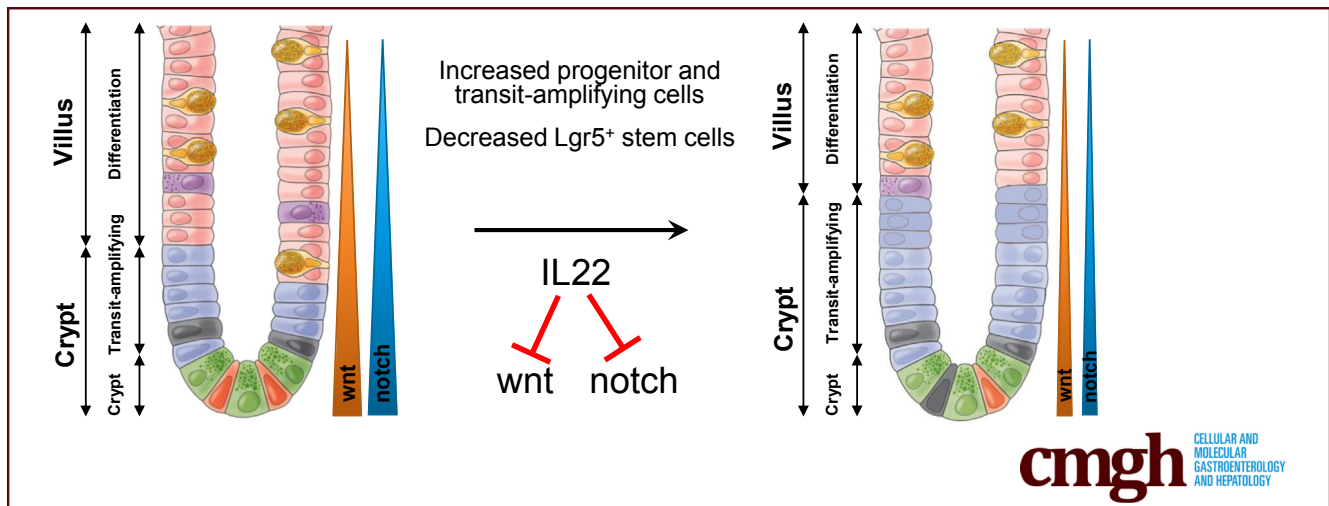


ORIGINAL RESEARCH

Interleukin 22 Expands Transit-Amplifying Cells While Depleting $Lgr5^+$ Stem Cells via Inhibition of Wnt and Notch Signaling

Juan-Min Zha,^{1,2,a} Hua-Shan Li,^{1,a} Qian Lin,^{1,a} Wei-Ting Kuo,³ Zhi-Hui Jiang,¹ Pei-Yun Tsai,² Ning Ding,¹ Jia Wu,¹ Shao-Fang Xu,¹ Yi-Tang Wang,² Jian Pan,⁴ Xiu-Min Zhou,¹ Kai Chen,¹ Min Tao,¹ Matthew A. Odenwald,² Atsushi Tamura,⁵ Sachiko Tsukita,⁵ Jerrold R. Turner,^{2,3,b} and Wei-Qi He^{1,2,b}

¹Jiangsu Key Laboratory of Neuropsychiatric Diseases and Cambridge-Suda (CAM-SU) Genome Resource Center, Soochow University, and Department of Oncology, First Affiliated Hospital of Soochow University, Suzhou, China; ²Department of Pathology, University of Chicago, Chicago, Illinois; ³Department of Pathology, Brigham and Women's Hospital and Harvard Medical School, Boston, Massachusetts; ⁴Institute of Pediatrics, Children's Hospital of Soochow University, Suzhou, China; and ⁵Laboratory of Biological Science, Graduate School of Frontier Biosciences and Graduate School of Medicine, Osaka University, Osaka, Japan



SUMMARY

IL22 promotes epithelial proliferation and mucosal repair. This is generally thought to reflect expansion of $Lgr5^+$ crypt base columnar intestinal stem cell populations. This study shows that IL22 depletes $Lgr5^+$ intestinal stem cells and promotes mucosal healing by enhancing proliferation of transit-amplifying cells.

BACKGROUND & AIMS: Epithelial regeneration is essential for homeostasis and repair of the mucosal barrier. In the context of infectious and immune-mediated intestinal disease, interleukin (IL) 22 is thought to augment these processes. We sought to define the mechanisms by which IL22 promotes mucosal healing.

METHODS: Intestinal stem cell cultures and mice were treated with recombinant IL22. Cell proliferation, death, and differentiation were assessed in vitro and in vivo by morphometric analysis, quantitative reverse transcriptase polymerase chain reaction, and immunohistochemistry.

RESULTS: IL22 increased the size and number of proliferating cells within enteroids but decreased the total number of enteroids. Enteroid size increases required IL22-dependent up-regulation of the tight junction cation and water channel claudin-2, indicating that enteroid enlargement reflected paracellular flux-induced swelling. However, claudin-2 did not contribute to IL22-dependent enteroid loss, depletion of $Lgr5^+$ stem cells, or increased epithelial proliferation. IL22 induced stem cell apoptosis but, conversely, enhanced proliferation within and expanded numbers of transit-amplifying cells. These changes were associated with reduced wnt and notch signaling, both in vitro and in vivo, as well as skewing of epithelial differentiation, with increases in Paneth cells and reduced numbers of enteroendocrine cells.

CONCLUSIONS: IL22 promotes transit-amplifying cell proliferation but reduces $Lgr5^+$ stem cell survival by inhibiting notch and wnt signaling. IL22 can therefore promote or inhibit mucosal repair, depending on whether effects on transit-amplifying or stem cells predominate. These data may explain why mucosal healing is difficult to achieve in some inflammatory bowel disease patients despite markedly elevated IL22

production. (*Cell Mol Gastroenterol Hepatol* 2019;7:255–274; <https://doi.org/10.1016/j.jcmgh.2018.09.006>)

Keywords: Interleukin 22; Enteroid; Intestinal Stem Cell; Transit-Amplifying Cell; Regeneration; wnt; notch; tight junction; claudin-2.

See editorial on page 409.

The intestinal epithelial barrier is essential for health. Both homeostatic maintenance and repair of this barrier rely on asymmetric division of intestinal stem cells (ISCs) to yield a stem cell and a transit-amplifying cell. The latter continues to proliferate while migrating out of the crypt, differentiates, and ultimately undergoes programmed cell death. These processes are regulated by intrinsic and extrinsic factors,^{1–3} including signals elaborated by immune cells. However, the mechanisms that govern ISC and transit-amplifying cell expansion in response to tissue injury and immune activation remain poorly understood.

In recent years interleukin 22 (IL22), a member of the IL10 family, has gained recognition as a driver of disease in rheumatoid arthritis and psoriasis.^{4–8} Although IL22 can also be pathogenic in some forms of enteric disease,^{9–12} it is more frequently beneficial and has been shown to promote epithelial proliferation, tissue regeneration, mucosal defense, and resolution of inflammation in immune-mediated and infectious intestinal disorders.^{13–18} In infectious enterocolitis, beneficial effects of IL22 include up-regulation of the tight junction protein claudin-2, which enhances paracellular water and Na⁺ flux to promote pathogen clearance.¹³ In most other contexts, the mechanisms by which IL22 regulates intestinal disease as well as the specific effects of IL22 on ISC and transit-amplifying cell function remain incompletely defined.

Here we sought to determine the impact of IL22 on ISC and transit-amplifying cell function *in vitro* and *in vivo*. IL22 increased the size of small intestinal enteroids in a claudin-2–dependent manner, indicating that claudin-2–mediated paracellular water flux is required for IL22-induced enteroid expansion. Transit-amplifying cell proliferation was also enhanced by IL22. Despite increases in enteroid size and epithelial proliferation, IL22 reduced enteroid number by a claudin-2–independent mechanism. Diminished enteroid survival was due to loss of Lgr5⁺ ISC that resulted from inhibition of wnt and notch signaling. These disparate effects on transit-amplifying and stem cells may explain the alternately beneficial and harmful, respectively, impact of IL22 signaling in mucosal disease.

Results

Interleukin 22 Augments Size But Reduces Survival of Freshly Derived Enteroids

Previous studies suggest that IL22 released by pericryptal group 3 innate lymphoid cells promotes ISC regeneration.^{19–21} To better characterize this process, mouse

jejunal crypts were isolated and cultured with recombinant IL22 (Figure 1A). Consistent with published work,²⁰ supplementation of epidermal growth factor, noggin, R-spondin (ENR) media with IL22 increased enteroid cross-sectional area (Figure 1B). A recent study has demonstrated that this also occurs in ileal-derived enteroids.²¹ This dose-dependent effect of IL22 was maximal at 5 ng/mL IL22, consistent with prior results,²⁰ and caused enteroid area to expand to 337% ± 42% of untreated controls ($P = .001$).

In contrast to increased size, IL22 markedly reduced enteroid numbers (Figure 1C). This effect of IL22 on enteroid numbers could be detected at IL22 doses as low as 0.1 ng/mL. At higher concentrations, IL22 reduced enteroid numbers by as much as 64% ± 2% ($P = .004$, Figure 1C). The negative effect of IL22 on enteroid numbers was even more dramatic when IL22-treated enteroids were passaged. Numbers of enteroids were dramatically decreased after 1 passage in IL22-containing media, and almost no enteroids survived the second passage in IL22-containing media (Figure 1D and E). These data indicate that despite increasing size, IL22 limits enteroid survival.

The data above are consistent with previous work showing that IL22 increases enteroid size but reduces survival after passaging.²⁰ However, previous work only detected a modest effect on survival, even at 10 ng/mL IL22. We therefore considered the possibility that our commercial source of IL22 (PeproTech, Rocky Hill, NJ) contained contaminants that limited stem cell survival relative to the IL22 used in the previous study (GenScript, Nanjing, China). To test this hypothesis, PeproTech IL22 was compared with 4 other commercial IL22 preparations. All tested preparations significantly increased enteroid size but reduced numbers of surviving enteroids (Figure 1F and G). Moreover, the dose-dependent effects of IL22 from all sources were quantitatively similar in terms of effects and enteroid size and survival (Figure 1F and G). These data exclude differences in potency as an explanation for the divergence between our results and previous work. Because 5 different IL22 preparations from 3 different suppliers are unlikely to contain similar contaminants, these data also indicate that the observed reductions in enteroid survival are mediated by IL22. To determine whether these IL22 effects were specific to jejunum, ileal crypts were isolated, cultured as enteroids, and treated with IL22 at various concentrations

^aAuthors share co-first authorship; ^bAuthors share co-senior authorship.

Abbreviations used in this paper: EGFP, enhanced green fluorescent protein; EdU, 5-ethynyl-2'-deoxyuridine; EGFR, epidermal growth factor receptor; ENR, epidermal growth factor, noggin, R-spondin; ERK, extracellular signal-regulated kinase; IL, interleukin; ISC, intestinal stem cell; MAPK, mitogen-activated protein kinase; PBS, phosphate-buffered saline; RT-PCR, reverse transcriptase polymerase chain reaction; WRN, wnt3a, R-spondin, noggin.

 Most current article

© 2019 The Authors. Published by Elsevier Inc. on behalf of the AGA Institute. This is an open access article under the CC BY-NC-ND license (<http://creativecommons.org/licenses/by-nc-nd/4.0/>).

2352-345X

<https://doi.org/10.1016/j.jcmgh.2018.09.006>

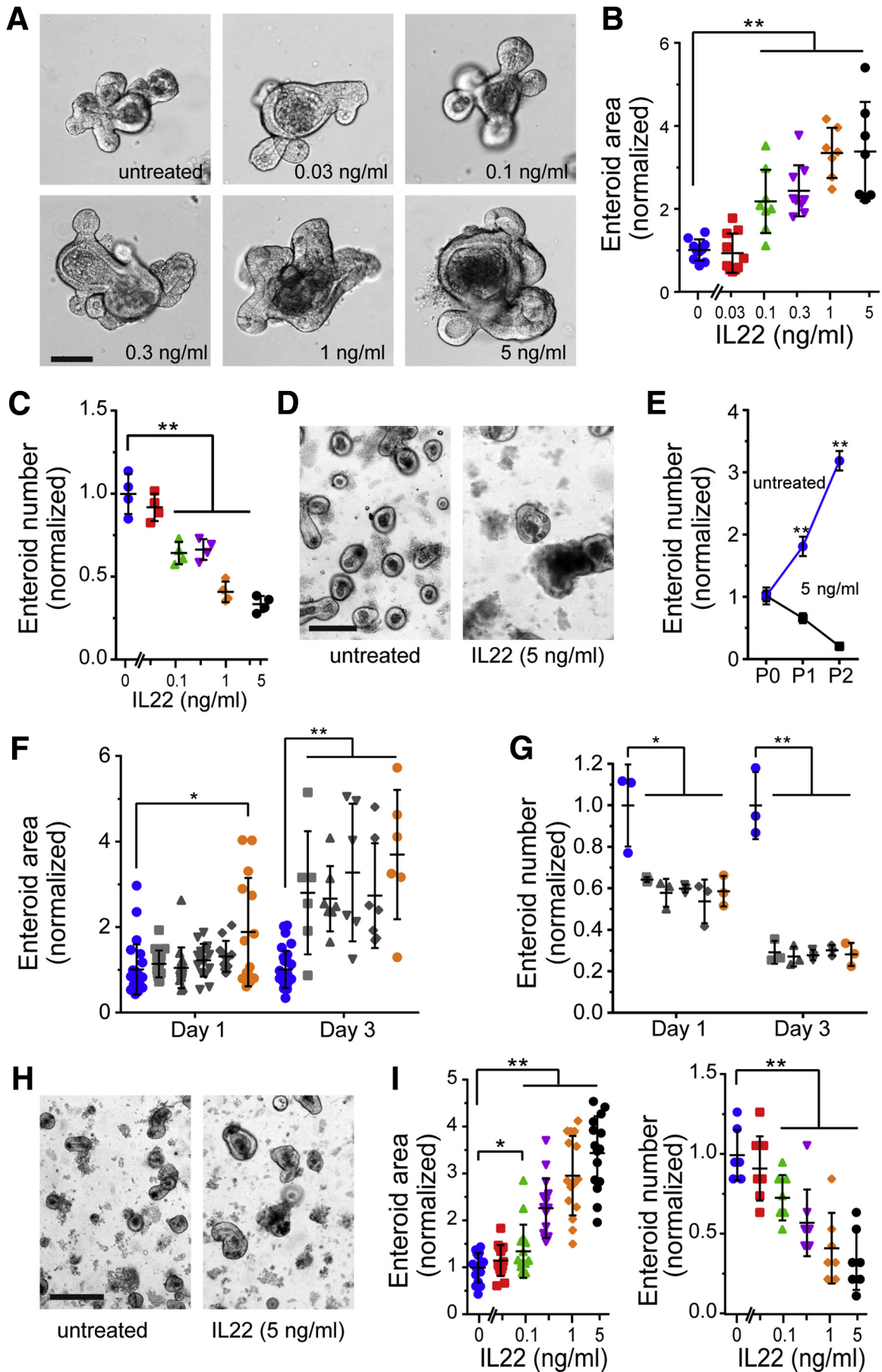


(Figure 1H and I). Results were similar to those in jejunal-derived enteroids, indicating that IL22 effects on enteroid size and survival are not region specific.

Interleukin 22 Effects on Size Require Claudin-2 Expression But Are Mechanistically Unrelated to Enteroid Survival

We have recently shown that IL22 potently induces expression of the tight junction protein claudin-2 within intestinal epithelial cells.¹³ Claudin-2 forms paracellular channels that enhance flux of Na⁺ and water.^{22–24} We therefore asked whether increases in volume induced by IL22 might reflect claudin-2-dependent increases in paracellular flux of cations and water into the enteroid lumen (Figure 2A). Treatment with either a nonselective Jak inhibitor or a specific Stat3 inhibitor prevented *Cldn2* transcriptional activation (Figure 2A). Morphologic examination showed that Jak or Stat3 inhibition also prevented increases in enteroid size (Figure 2B and C) and improved enteroid survival (Figure 2C). These data suggest that claudin-2 up-regulation may be required for IL22-induced effects on enteroid size. However, these pharmacologic inhibitors are not specific for claudin-2 because they block many components of IL22 signaling.

To overcome the limitations of pharmacologic inhibitors, we isolated enteroids from wild-type, claudin-2 transgenic, and claudin-2 knockout mice. The size of enteroids derived from wild-type and claudin-2 transgenic mice was similarly increased by IL22, but IL22 did not increase the size of claudin-2 knockout enteroids (Figure 2D and E). In contrast, IL22 caused similar reductions in numbers of wild-type, claudin-2 knockout, and claudin-2 transgenic enteroids (Figure 2F). Thus, IL22-induced effects on size, but not survival, require claudin-2 expression. These data suggest that IL22-induced increases in enteroid size are due to claudin-2-dependent paracellular water and cation flux and the resulting accumulation of luminal fluid. Moreover, IL22-induced increases in epithelial proliferation were similar in wild-type, claudin-2 knockout, and claudin-2 transgenic enteroids (Figure 2G). Thus, despite some controversy in the literature, these in vitro data confirm previous in vivo analyses of our claudin-2 transgenic mice and claudin-2

knockout mice that failed to show any perturbation of epithelial proliferation or turnover.^{13,25,26}

Interleukin 22 Induces Epithelial Apoptosis In Vitro

To better define the mechanisms by which IL22 reduced enteroid numbers, we initially assessed the morphologic changes induced by IL22. Most enteroids were viable after IL22 treatment, but we did note peripheral granulated cells. These cells took up propidium iodide, consistent with cell death (Figure 3A). Moreover, caspase 3/7 activation was significantly increased by IL22 treatment (Figure 3B). IL22 treatment therefore induces epithelial apoptosis in vitro.

Interleukin 22 Reduces Numbers of Lgr5⁺ Stem Cells In Vitro

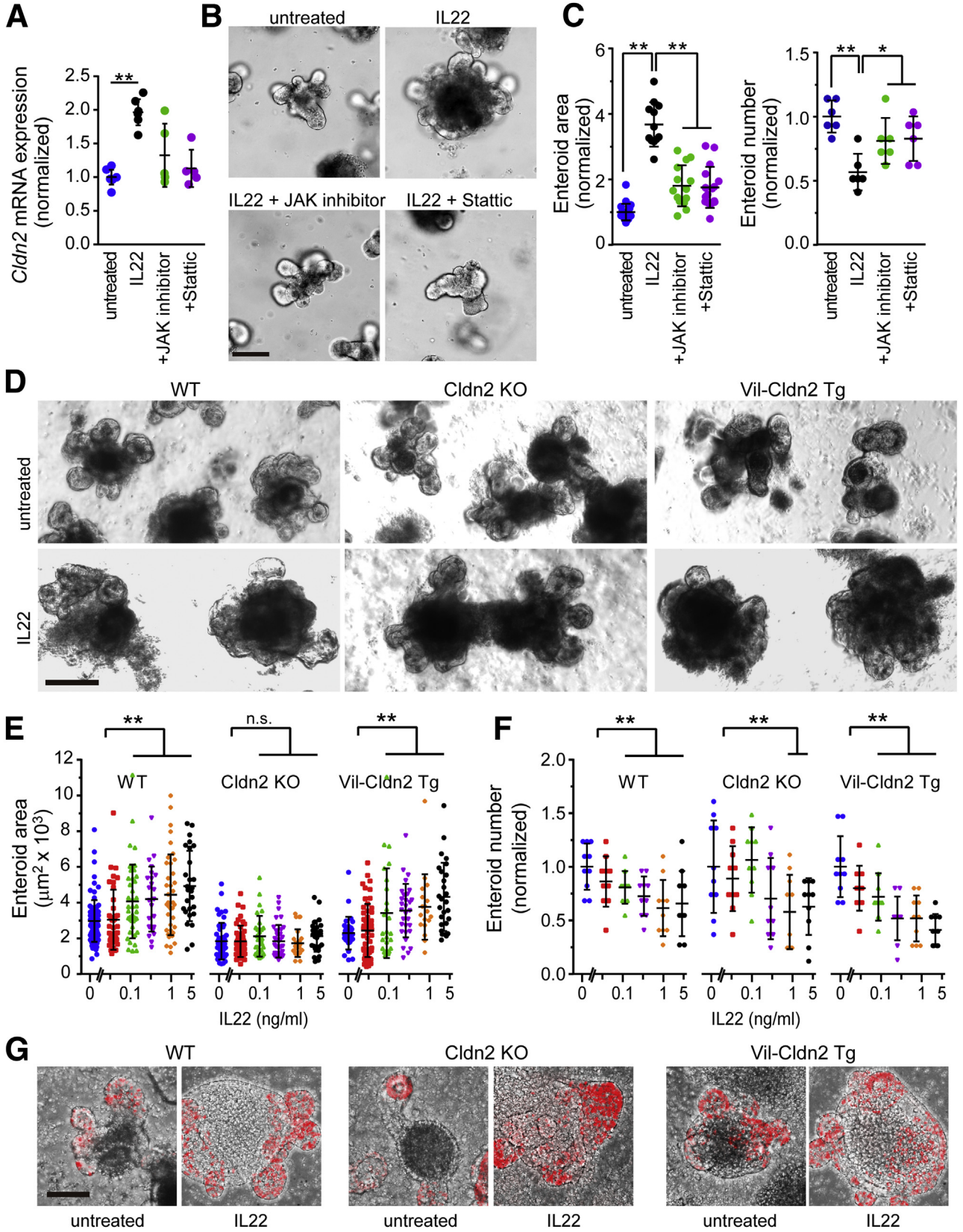
To directly assess the effects of IL22 on survival of Lgr5⁺ stem cells, jejunal crypts were isolated from Lgr5-EGFP-IRES-CreER^{T2} mice. In the absence of IL22, most enteroids contained multiple enhanced green fluorescent protein (EGFP)⁺ stem cells (Figure 4A) despite the known mosaicism of expression in these mice. In contrast, few EGFP⁺ ISCs were detected in IL22-treated enteroids (Figure 4A). When analyzed by flow cytometry, there was a 5-fold reduction in the number of Lgr5-EGFP⁺ cells within these enteroids (Figure 4B).

Consistent with loss of active Lgr5⁺ stem cells, mRNA expression of *Lgr5* and the stem cell markers *Ascl2*, *Olfm4*, and *Sox9*^{27,28} was also significantly down-regulated in IL22-treated enteroids (Figure 4C). This reduction was limited to active ISCs, because reserve stem cell markers *Bmi1*, *Hopx*, *Tert*, and *Trig1*^{2,28–32} were not affected by IL22 treatment (Figure 4D). These data suggest that IL22 specifically depletes the Lgr5⁺, active stem cell pool.

Interleukin 22 Reduces Lgr5⁺ Stem Cell Numbers and Intestinal Stem Cell Proliferative Capacity In Vivo

To determine whether IL22 limits ISC proliferation in vivo, crypts were isolated from mice that had been treated with IL22 (1 μg/day) for 7 days. Although IL22 was not included in the culture media, enteroid recovery from isolated crypts was markedly reduced by in vivo IL22 exposure

Figure 1. (See previous page). IL22 increases size, but reduces numbers, of jejunal- and ileal-derived enteroids. (A) Bright-field images of freshly derived jejunal enteroids cultured in ENR supplemented with a range of IL22 concentrations (0.03, 0.1, 0.3, 1, and 5 ng/mL; PeproTech) for 3 days. Images are representative of more than 5 independent experiments. Bar, 100 μm. **(B)** Quantification of jejunal enteroid cross-sectional area after culture for 3 days. Each point indicates the mean area of 20–30 enteroids in a single well. n = 7–10 in this experiment, which is representative of more than 5 independent experiments. **P < .01. **(C)** Quantification of jejunal enteroid number after 3 days of culture in ENR with IL22. Each point indicates the number of enteroids in a single well. n = 4 in this experiment, which is representative of more than 3 independent experiments. **P < .01. **(D)** Enteroids after being passaged once in ENR without or with IL22 (5 ng/mL, PeproTech). Bright-field images were taken 1 day after passaging. Bar, 200 μm. **(E)** Quantification of enteroid survival and expansion during serial passaging without or with IL22 (PeproTech). Each point indicates the mean number of enteroids from 4 wells. Data are representative of 3 independent experiments. **P < .01. **(F and G)** Quantification of cross-sectional area and number of jejunal enteroids cultured for 1 or 3 days with IL22 from different commercial sources (1 ng/mL). Blue symbols indicate enteroids cultured without IL22. Sources of IL22, from left to right, were GenScript Z03350, GenScript Z02197, R&D 582ML-010, R&D 582ML-010/CF, and PeproTech 201-22 (gold symbols). Each point indicates enteroid area (n = 6–25) or total number of enteroids in a single well (n = 3). Data are representative of 3 independent experiments. *P < .05, **P < .01. **(H)** Ileal enteroids were cultured in ENR without or with IL22 (5 ng/mL, PeproTech) for 1 day. Bar, 200 μm. **(I)** Quantification of ileal enteroid cross-sectional area (n = 15) and number (n = 7) after culture for 3 days with IL22 (1 ng/mL, PeproTech). Data are representative of 3 independent experiments. *P < .05, **P < .01.



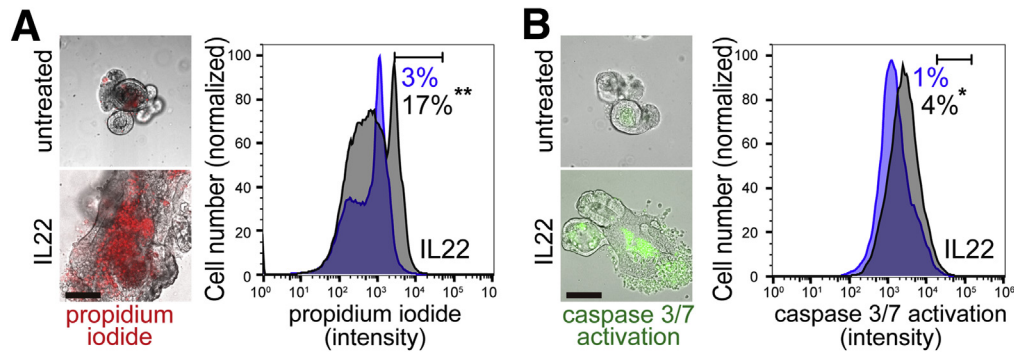


Figure 3. IL22 promotes cell death. (A) Merged bright-field and fluorescent images and flow cytometric analysis of enteroids cultured in ENR without or with IL22 (5 ng/mL, PeproTech) for 3 days and stained with propidium iodide (red in images). Histograms of flow cytometry data from enteroids cultured without (blue) or with (black) IL22. Fractions of cells within the window are indicated. Data are representative of 3 separate analyses. Bar, 100 μ m. ****** $P < .01$. (B) Merged bright-field and fluorescent images and flow cytometric analysis of enteroids cultured in ENR without or with IL22 (5 ng/mL, PeproTech) for 3 days and labeled for caspase 3/7 activation (green in images). Histograms of flow cytometry data from enteroids cultured without (blue) or with (black) IL22. Fractions of cells within the window are indicated. Data are representative of 3 separate analyses. Bar, 100 μ m. ***** $P < .05$.

(Figure 5A and B). Nevertheless, the area of the enteroids generated from IL22-treated mice was increased relative to those from saline-injected mice (Figure 5C). In vivo IL22 treatment therefore reduces ex vivo epithelial survival and proliferative capacity but promotes formation of larger enteroids. These data demonstrate that the changes induced by in vitro IL22 treatment also occur in vivo and are durable.

To directly assess the active stem cell compartment in vivo, expression of *Lgr5*, *Olfm4*, and *Ascl2* was assessed in crypts isolated from saline- and IL22-treated mice. Similar to in vitro IL22 treatment, in vivo treatment reduced *Lgr5*, *Ascl2*, and *Olfm4* expression (Figure 5D). In vivo IL22 treatment also reduced numbers of *Lgr5*-EGFP-expressing (Figure 5E) and *Olfm4*-expressing (Figure 5F) cells within jejunal crypts. Similar changes occurred in ileal mucosae (Figure 5G and H). Overall, these data show that similar to in vitro treatment, IL22 reduces numbers and proliferative potential of active, *Lgr5*⁺ intestinal stem cells in vivo.

Interleukin 22 Stimulates Epithelial Proliferation In Vitro and In Vivo

Our observation that IL22 treatment reduces stem cell numbers conflicts with a previous report.²⁰ To better understand this discrepancy, DNA synthesis was tracked as a marker of intestinal epithelial proliferation. Incorporation of the uridine analog 5-ethynyl-2'-deoxyuridine (EdU) was markedly

increased by IL22 (Figure 6A, $P < .001$). Despite reduced expression of *Lgr5* ISC markers (Figure 4C), expression of the proliferative marker Ki67, the stem and transit-amplifying cell marker *Prom1*/CD133, the transit-amplifying cell marker *Zfp652*, and the immature enterocyte marker *Prss32* were all increased by IL22 treatment in vitro (Figure 6B). These observations suggest that IL22 expands the transit-amplifying cell compartment. Consistent with this, in vivo IL22 treatment significantly increased crypt depth and numbers of Ki67-positive epithelial cells per crypt within jejunum (Figure 6C) and ileum (Figure 6D). Another study performed contemporaneously with this work and reported in the previous issue of CMGH has also demonstrated reduced ileal epithelial proliferation, in vitro and in vivo, in response to IL22.²¹

Although the in vivo data correlate perfectly with the in vitro studies of isolated epithelial cells, we considered the possibility that in vivo IL22 treatment recruits local immune cells that alter intestinal epithelial signaling. However, we did not detect changes in T-cell, macrophage, or granulocyte, ie, neutrophil, numbers by either morphologic examination or quantitative reverse transcriptase polymerase chain reaction (RT-PCR) (Figure 6E).

Interleukin 22 Inhibits wnt Signaling

Wnt signaling is critical for ISC maintenance.^{2,27,33} We therefore asked whether IL22-induced ISC loss reflected

Figure 2. (See previous page). IL22-induced increases in enteroid size require claudin-2 up-regulation. (A) *Cldn2* mRNA expression in jejunal enteroids cultured in ENR without or with IL22 (1 ng/mL, Peprotech), JAK inhibitor (JAK inhibitor I, 0.5 μ mol/L), or STAT3 inhibitor (stattic, 5 μ mol/L) for 3 days. $n = 5$ in this representative experiment. (B and C) Bright-field images, cross-sectional area ($n = 12$ –20), and number ($n = 6$) of jejunal enteroids after culture for 3 days with IL22 (1 ng/mL, PeproTech), JAK inhibitor I, or stattic. Bar, 100 μ m. ***** $P < .05$, ****** $P < .01$. (D) Bright-field images of jejunal enteroids from wild-type (WT), claudin-2 knockout (*Cldn2* KO), and claudin-2 transgenic (*Vil-Cldn2* Tg) mice cultured in ENR without or with IL22 (1 ng/mL, PeproTech) for 3 days. Bar, 200 μ m. Images are representative of 3 independent experiments. (E and F) Cross-sectional area ($n = 16$ –90) and number ($n = 10$) of jejunal enteroids derived from wild-type (WT), claudin-2 knockout (*Cldn2* KO), and claudin-2 transgenic (*Vil-Cldn2* Tg) mice after 3 days of culture with indicated IL22 concentrations. Data are representative of 3 independent experiments. ****** $P < .01$. (G) Morphologic analysis of EdU (red) incorporation into enteroids derived from wild-type (WT), claudin-2 knockout (*Cldn2* KO), and claudin-2 transgenic (*Vil-Cldn2* Tg) mice during 2-hour EdU pulse after 3 days of culture without or with IL22 (5 ng/mL). Bar, 100 μ m. Representative data are shown.

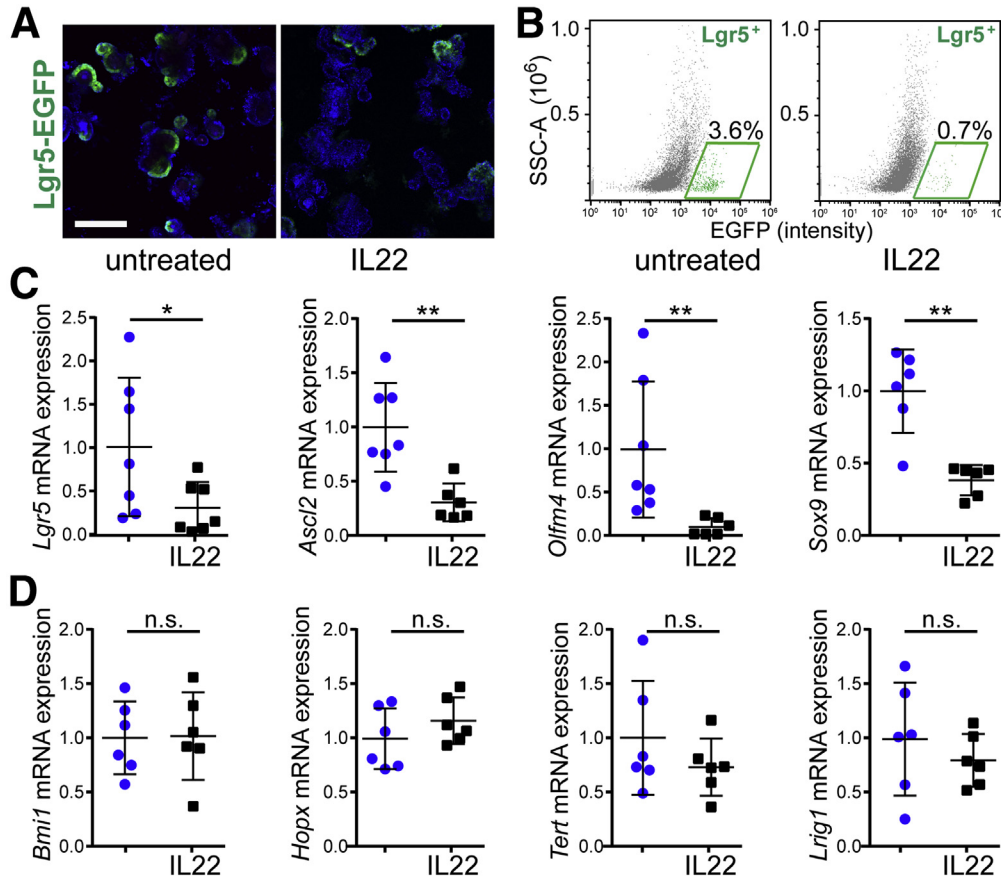


Figure 4. IL22 reduces $Lgr5^+$ ISC numbers and expression of active ISC markers in vitro. (A) Jejunal enteroids from $Lgr5$ -EGFP-IRES-CreER^{T2} mice were cultured in ENR without or with IL22 for 3 days (5 ng/mL, PeproTech) and stained with Hoechst 33342 (blue). Images are representative of more than 3 independent experiments. Bar, 200 μ m. (B) Flow cytometric analyses of $Lgr5$ -EGFP-IRES-CreER^{T2} enteroids cultured in ENR without (left) or with (right) IL22 (5 ng/mL, PeproTech) for 3 days. Fractions of $Lgr5^+$ cells within the designated windows are shown. $P < .05$. Data are representative of more than 3 independent experiments. (C and D) Quantitative RT-PCR analysis of relative mRNA expression in jejunal enteroids cultured in ENR without (blue symbols) or with (black symbols) IL22 (5 ng/mL, PeproTech; $n = 6-7$ in the representative experiments shown). * $P < .05$, ** $P < .01$.

suppression of wnt signaling. In vitro IL22 treatment did not affect transcription of *Wnt3* or wnt receptors *Lrp5* and *Lrp6* (Figure 7A). However, expression of the wnt antagonist *Dkk1* was increased by IL22, and expression of the *Fzd7* wnt receptor was reduced (Figure 7B). This appeared to be sufficient to inhibit wnt signaling, because expression of wnt target genes *Axin2*, *Cmyc*, and *Cd44* was also reduced after in vitro IL22 treatment (Figure 7C).²¹ In vivo IL22 treatment had similar effects on *Dkk1*, *Axin2*, and *Cmyc* expression (Figure 7D), confirming that the results are not an artifact of the in vitro culture system. Finally, in vivo IL22 treatment markedly reduced the number of beta-catenin positive epithelial nuclei within crypt and transit-amplifying regions, consistent with reduced wnt signaling (Figure 7E and F).

Exogenous wnt Is Unable to Overcome Interleukin 22-Induced Growth Suppression

The data above indicate that wnt signaling is reduced in IL22-treated enteroids grown in ENR media, ie, media

without exogenous wnt. We considered the hypothesis that increased wnt activity driven by exogenous wnt could rescue enteroids from IL22-induced ISC loss. To test this idea, enteroids were cultured in wnt3a, R-spondin, noggin (WRN) media.³⁴ As expected, this increased the size of enteroids and caused them to assume spheroid shapes, without crypt-like buds.^{3,34} In contrast to enteroids cultured in ENR, IL22 treatment markedly reduced spheroid size during culture in WRN (Figure 8A and B). These increases were similar at 1 ng/mL and 5 ng/mL IL22, but there was a dose-dependent effect of IL22 on enteroid/spheroid survival in WRN media (Figure 8C) that was similar to effects in ENR media. The reductions in enteroid size were not related to failure of claudin-2 up-regulation, because IL22 induced *Cldn2* transcription in spheroids grown in WRN media (Figure 8D). In contrast, IL22 reduced expression of the proliferative markers *Ki67* and *Pcna* (Figure 8E and F). Consistent with reduced proliferation, EdU incorporation was also markedly reduced by IL22 treatment of spheroids (Figure 8G). This reduced proliferation likely explains the

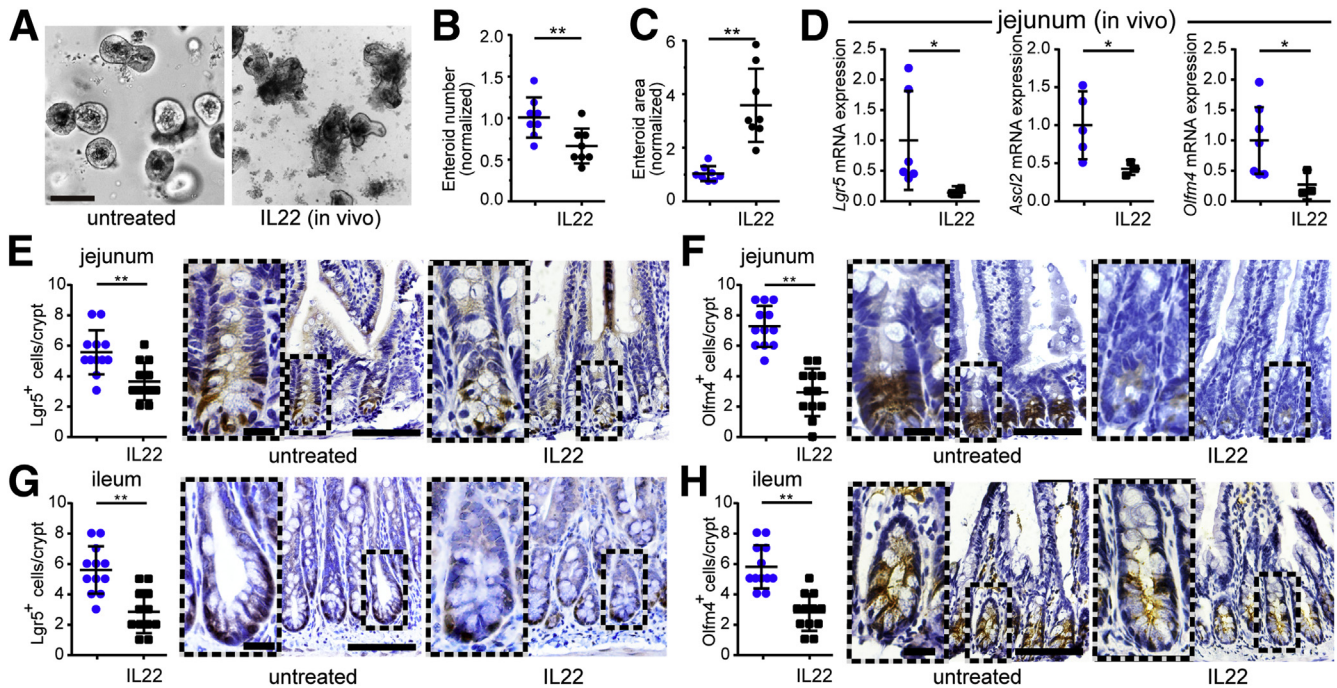


Figure 5. IL22 reduces *Lgr5*⁺ stem cell numbers in vivo. (A) Mice were treated with IL22 (1 μ g/day for 7 consecutive days). Tissues were collected on day 8. Isolated jejunal crypts were grown as enteroids in ENR medium without added IL22. Bright-field images after 2 days of culture are shown. Images are representative of 3 independent experiments. Bar, 100 μ m. (B and C) Enteroid cross-sectional area (n = 8) and number (n = 8) were quantified. **P* < .05, ***P* < .01. (D) Quantitative RT-PCR of relative mRNA expression in isolated jejunal epithelium. n = 3–7 in the representative experiment shown. **P* < .05. (E and F) *Lgr5*-EGFP (detected using anti-GFP) and *Olfm4* immunostains of jejunal tissue sections from IL22- or saline-treated mice. Numbers of positive cells per well-oriented crypt are shown. Each point (n = 12) represents a separate field from a total of 5–7 mice per condition. Bar, 100 μ m. Bar, 20 μ m (insets). ***P* < .01. (G and H) *Lgr5*-EGFP and *Olfm4* immunostains of ileal tissue sections from IL22- or saline-treated mice. Numbers of positive cells per well-oriented crypt are shown. Each point (n = 12) represents a separate field from a total of 5–7 mice per condition. Bar, 100 μ m. Bar, 20 μ m (insets). ***P* < .01.

smaller size of spheroids grown in WRN media and treated with IL22. These data indicate that IL22-induced up-regulation and down-regulation of *Dkk1* and *Fzd7*, respectively (Figure 7B and D), rather than insufficient wnt ligand, are responsible for the observed reductions in wnt signaling.

Interleukin 22 Inhibits Notch Signaling and Skews Epithelial Cell Differentiation

Notch is closely intertwined with wnt in regulating ISC maintenance and direction of ISC differentiation.^{35–39} Because of the disruption of wnt signaling induced by IL22, we asked whether notch effectors and signaling were perturbed by IL22. Transcription of notch ligands *Dll1* and *Jagged1*, but not *Dll4*, as well as the notch receptor *Notch1*, were all reduced in IL22-treated enteroids (Figure 9A). Similarly, mRNA expression of the notch target *Hes1* was attenuated by IL22 (Figure 9A). Similar results were obtained in vivo, where IL22 treatment reduced transcription of *Dll1*, *Jagged1*, *Notch1*, and *Hes1* (Figure 9B). Furthermore, immunohistochemistry and morphometric analyses documented reduced numbers of nuclei that were positively stained for the notch intracellular domain (Figure 9C). Further evidence of IL22-induced down-regulation of notch

signaling in vitro and in vivo is provided by reduced transcription of mature enterocyte markers (Figure 10A and B). These data therefore indicate that in addition to inhibiting wnt signaling, IL22 disrupts notch signaling.

Inhibition of both notch and wnt signaling suggests that IL22 may increase goblet cell numbers.³⁵ However, there were no changes in expression of transcripts for the goblet cell markers *Muc2*, *Spink4*, or *Atoh1* or numbers of MUC2-expressing cells in vitro (Figure 11A). Similarly, IL22 did not affect *Muc2* transcription or numbers of MUC2-expressing cells in vivo (Figure 12A).

IL22 increased transcription of Paneth cell markers *Lyz1*, *Mmp7*, *Reg3b*, and *Reg3g* and numbers of lysozyme-expressing cells in vitro (Figure 11B) and in vivo (Figure 12B). This increase in Paneth cell numbers could be consistent with reduced but continued wnt signaling along with more substantial notch inhibition.^{35,40}

One recent study suggests that simultaneous inhibition of wnt and notch signaling may promote enteroendocrine cell differentiation.⁴¹ However, IL22 treatment reduced expression of *ChgA*, *ChgB*, and *Neurog3* transcripts as well as numbers of chromogranin A-positive cells in vitro (Figure 11C) and in vivo (Figure 12C). This result was unexpected because wnt and notch signaling were both suppressed by IL22. However, it has been reported that

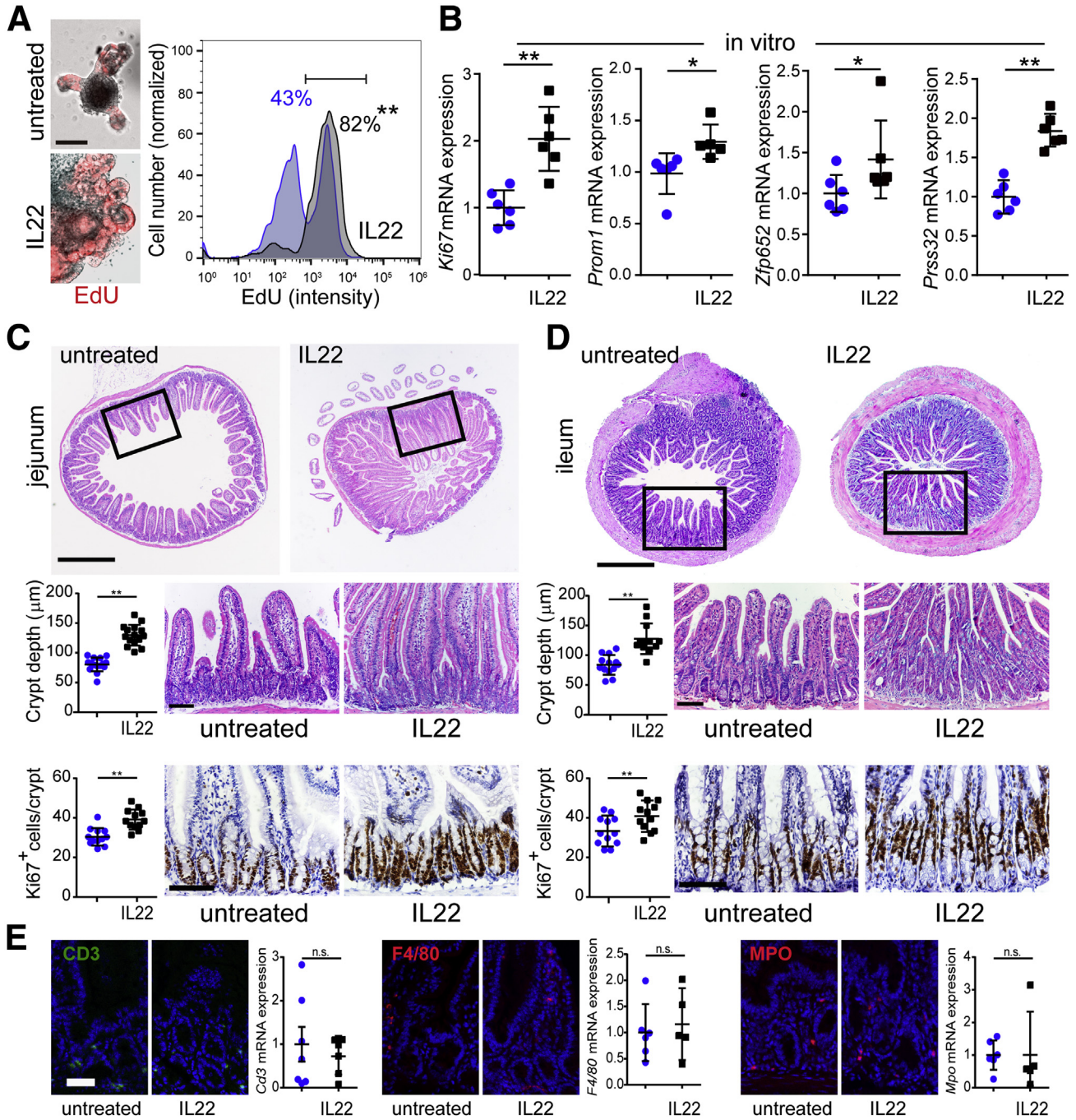


Figure 6. IL22 increases epithelial proliferation in vitro and in vivo. (A) Jejunal enteroids were cultured in ENR without or with IL22 (5 ng/mL, PeproTech) for 3 days and then pulsed with EdU (red) for 1 hour before fixation. Bar, 100 μ m. Histograms of flow cytometry data from enteroids cultured without (blue) or with (black) IL22 are shown, along with the fraction of cells within the indicated window. Data are representative of 3 separate analyses. $^{**}P < .01$. (B) Relative mRNA expression of *Ki67* (proliferative marker), *Prom1* (stem- and transit-amplifying cell marker), *Zfp652* (transit-amplifying cell marker), and *Prss32* (immature enterocyte marker) in jejunal enteroids cultured without (blue symbols) or with IL22 (black symbols) (5 ng/mL, PeproTech; in ENR.) $n = 5-6$ in the representative experiment shown. $^{*}P < .05$, $^{**}P < .01$. (C and D) Jejunal (C) and ileal (D) sections from mice treated with saline or IL22 (as in Figure 5) were stained by hematoxylin-eosin or immunostained for Ki67. Representative complete cross sections (H&E) are shown along with higher magnification images and depth of well-oriented crypts ($n = 12$). Numbers of positive cells per crypt were assessed in Ki67 immunostains. Bars, 500 μ m (upper images), 100 μ m (higher magnification H&E and immunostain images). For all graphs, each point ($n = 12$) represents a separate field of view from a total of 5-7 mice per condition. Representative data are shown. $^{**}P < .01$. (E) Snap-frozen jejunum from IL22- or saline-treated mice was immunostained for CD3, F4/80, or myeloperoxidase (MPO) to assess infiltrates of lymphocytes, macrophages, and granulocytes, respectively. Relative mRNA expression of *Cd3*, *F4/80*, and *Mpo* in jejunum isolated from saline- and IL22-treated mice is shown. $n = 5-7$. IL22 did not induce influx of any immune cell population. Bar, 50 μ m.

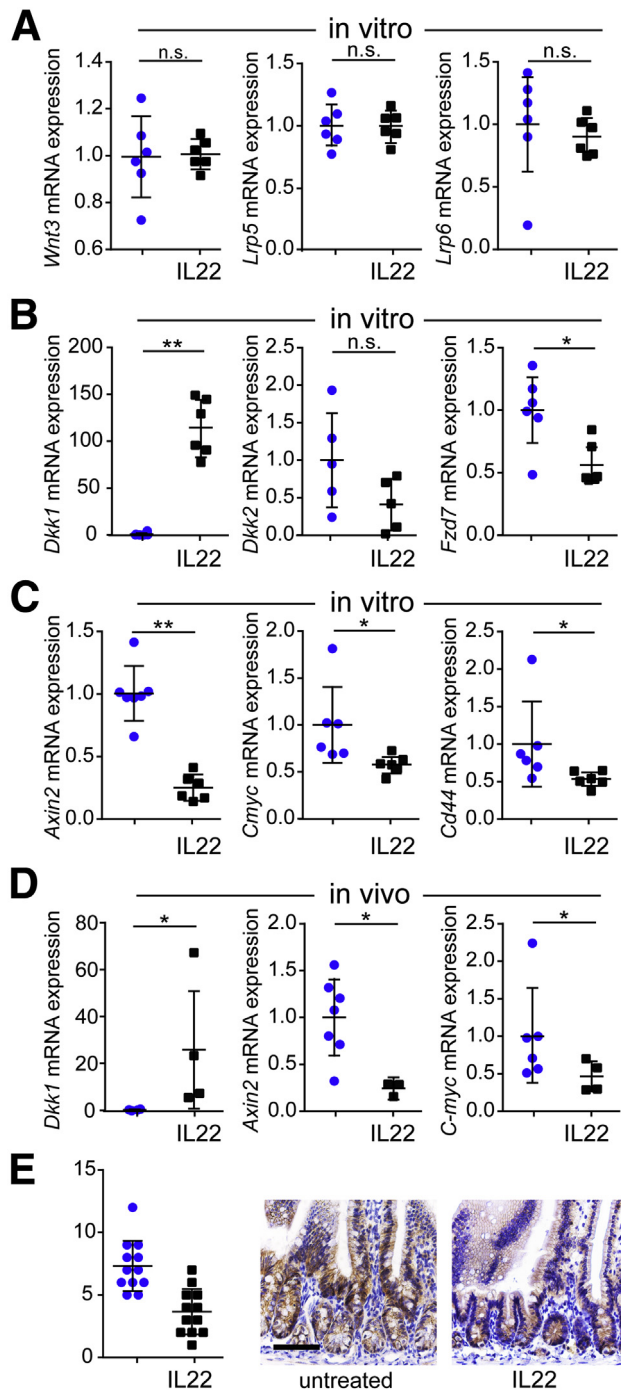


Figure 7. IL22 inhibits wnt signaling in vitro and in vivo. (A–C) Relative mRNA expression of *Wnt3*, *Lrp5*, *Lrp6*, *Dkk1*, *Dkk2*, *Fzd7*, *Axin2*, *C-myc*, and *Cd44* in jejunal enteroids cultured without (blue symbols) or with IL22 (black symbols) (5 ng/mL, PeproTech) in ENR for 3 days. $n = 6$ in the representative experiments shown. * $P < .05$; ** $P < .01$. (D) Quantitative RT-PCR of *Dkk1*, *Axin2*, and *C-myc* mRNA expression in isolated jejunal epithelium. $n = 3$ –7 in the representative experiment shown. * $P < .05$. (E) Immunostains and quantitative analysis of beta-catenin labeling in small intestine from untreated or IL22-treated mice. $n = 12$ fields from 5 mice. Bar, 100 μm .

simultaneous inhibition of wnt and notch along with blockade of epidermal growth factor receptor (EGFR) or mitogen-associated protein kinase (MAPK) signaling promotes enteroendocrine differentiation.⁴¹ We therefore asked whether, despite reducing wnt and notch signaling, IL22-induced augmentation of EGFR/MAPK signaling could explain reduced endocrine cell numbers. IL22 induced increases in EGFR and extracellular signal-regulated kinase (ERK), the MAPK downstream of EGFR, phosphorylation in vivo (Figure 12D and E). Notably, the epithelial cells with increased EGFR and ERK phosphorylation were within the zone where IL22-induced increases in proliferation and Ki67 expression were observed (Figure 6C). These data suggest that IL22-induced EGFR and ERK activation may be responsible for both increased transit-amplifying cell proliferation and reduced endocrine cell differentiation despite inhibition of wnt and notch signaling.

Discussion

Intestinal inflammation can lead to mucosal injury and impaired epithelial regeneration, but it can also promote healing. These effects can be mediated by direct immune-epithelial cell interactions or by secretion of effector molecules, eg, cytokines and growth factors. We show here that one secreted molecule, IL22, promotes both injury and regeneration. This may explain the observation that, despite increased IL22 expression, mucosal regeneration and healing are impaired in Crohn's disease patients.^{14,42} These results may also explain the inconsistent effects of IL22 therapy in experimental colitis.^{10,11,15,42–44}

In the small intestinal crypt, *Lgr5*⁺ ISCs are the actively cycling crypt base columnar cells. In contrast to previous work,²⁰ our data indicate that IL22 induces loss of *Lgr5*⁺ ISCs. Nevertheless, IL22 did increase epithelial proliferation, as indicated by increased numbers of EdU-positive cells in enteroids and expansion of the Ki-67 positive proliferative zone and crypt depth in vivo. These changes were accompanied by increased expression of transit-amplifying and immature enterocyte markers, ie, *Prom1/Cd133*, *Zfp652*, and *Prss32*.⁴⁵ The loss of *Lgr5*⁺ stem cells along with increased overall proliferation could reflect disruption of the normal asymmetrical divisions that preserve *Lgr5*⁺ stem cells while generating transit-amplifying cells. For example, it is plausible to hypothesize that IL22 promotes division of *Lgr5*⁺ stem cells to produce two transit-amplifying cells.⁴⁶ Zwarycz et al²¹ recently reached a similar conclusion. Alternatively, inhibition of notch signaling and down-regulation of *Dll1* may contribute to the loss of *Lgr5*⁺ cells, because *Dll1*-dependent notch signaling is required for intestinal stem cell homeostasis.⁴⁷ Moreover, *Dll1*-expressing epithelial cells are able to convert into and replenish pools of *Lgr5*⁺ stem cells in vitro and in vivo.^{40,48} Although we did not follow recovery of mice after IL22 treatment, it is likely that this restoration of actively cycling stem cell pools occurred, either from *Lgr5*⁺ cells or from

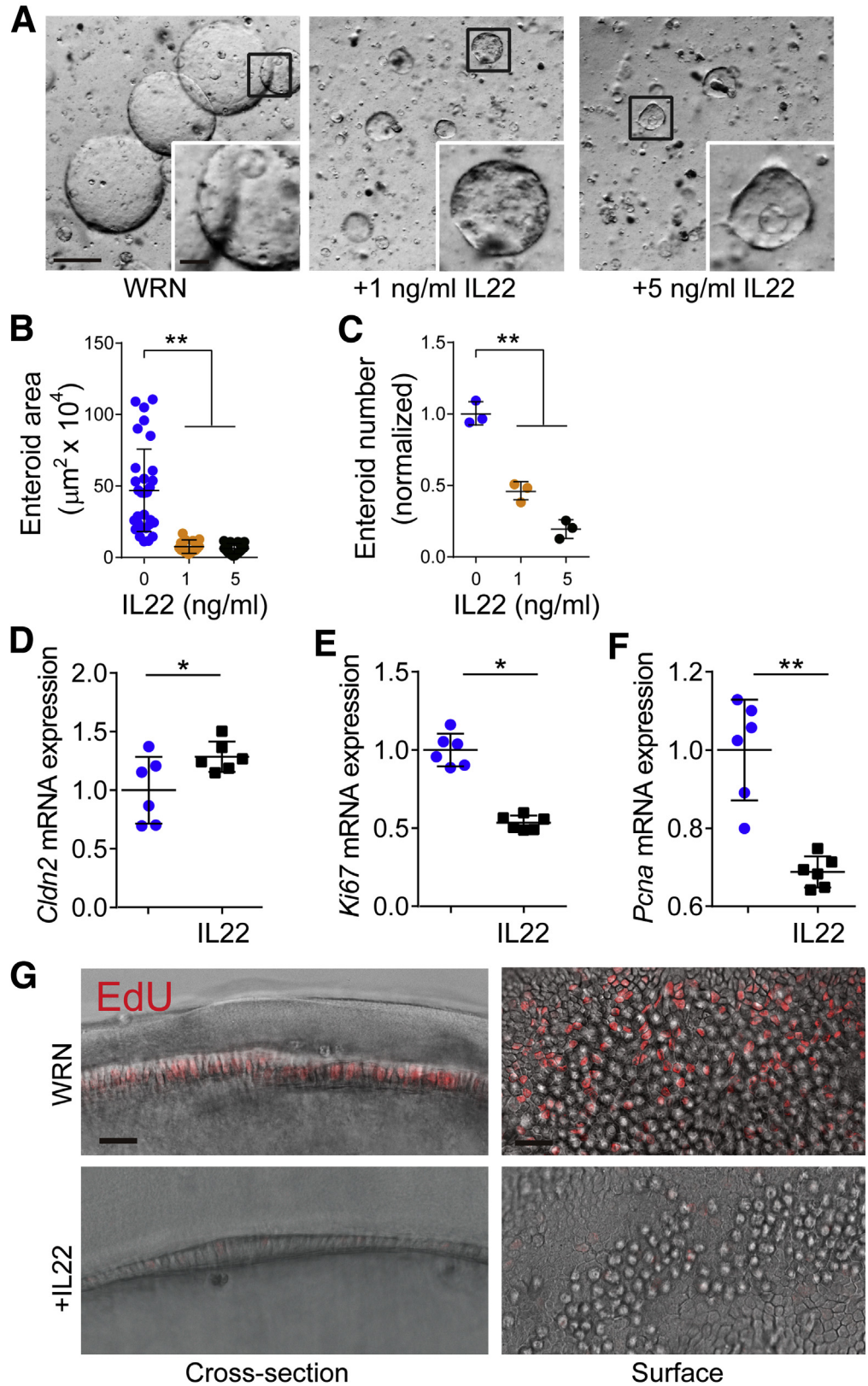


Figure 8. IL22 effects on enteroid size and number are resistant to rescue by exogenous wnt. (A) Jejunal enteroids were cultured in WRN without or with IL22 (1 or 5 ng/mL) for 4 days. Representative images are shown. Bar, 500 μm and 200 μm (insets). (B and C) Quantification of cross-sectional area ($n = 20-30$) and number ($n = 3$) of jejunal enteroids cultured in WRN with indicated concentrations of IL22. (D) *Cldn2* mRNA expression in enteroids (spheroids) cultured in WRN without (blue symbols) or with IL22 (black symbols) (5 ng/mL, PeproTech). $*P < .05$. (E and F) *Ki67* and *Pcna* expression was markedly reduced in IL22-treated spheroids. Data are representative of at least 3 independent experiments. $*P < .05$, $**P < .01$. (G) Jejunal enteroids were cultured in WRN without or with IL22 (5 ng/mL, PeproTech) for 3 days and then pulsed with EdU (red) for 1 hour before fixation. Bar, 25 μm .

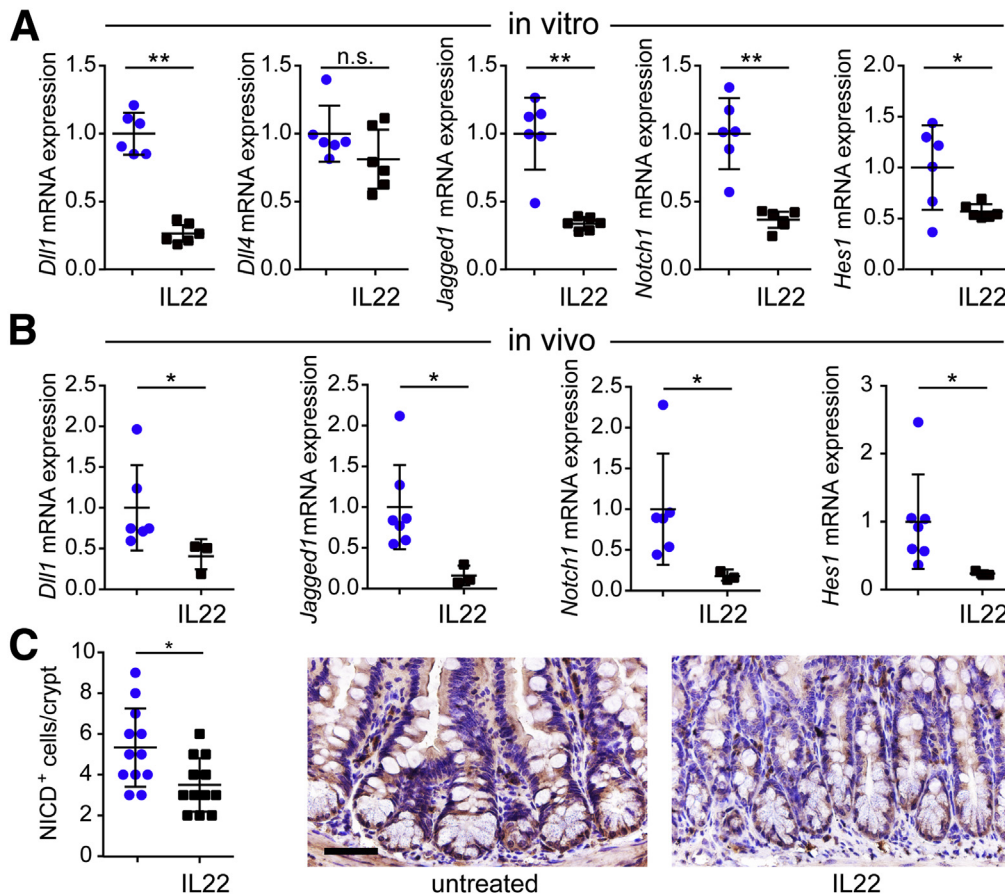


Figure 9. IL22 inhibits notch signaling and disrupts enterocyte maturation in vitro and in vivo. (A) Relative mRNA expression of notch pathway markers *Dll1*, *Dll4*, *Jagged-1*, *Notch1*, and *Hes1* in jejunal enteroids cultured in ENR without (blue symbols) or with IL22 (black symbols) (5 ng/mL, PeproTech) for 3 days. $n = 6$ in the representative experiments shown. $*P < .05$; $**P < .01$. (B) Relative mRNA expression of notch pathway markers in jejunal epithelial cells isolated from untreated and IL22-treated mice. $n = 3-7$ in the representative experiment shown. $*P < .05$. (C) Immunostains and quantitative analysis of notch intracellular domain (NICD) labeling in small intestine from untreated or IL22-treated mice. $n = 12$ fields from 5 mice. Bar, 50 μm .

the relatively non-proliferative pool of *Lgr5*⁺ cells,⁴⁸ after treatment ended.

A previous report noted that IL22 increased the size of small intestinal enteroids.²⁰ This was interpreted as enteroid growth due to IL22-induced increases in epithelial proliferation. However, it is now recognized that IL22 up-regulates expression of the tight junction pore protein claudin-2, which forms paracellular channels that transport cations and water.^{13,22,23,49-51} We therefore considered the possibility that increased enteroid size was due to luminal expansion rather than epithelial growth. This hypothesis is supported by work showing that zebrafish deficient in claudin-15, which forms a paracellular cation channel, fail to develop a gut lumen because of insufficient luminal fluid accumulation.⁵² Furthermore, although three-dimensional epithelial cysts grown from high resistance MDCK I cells, which have relatively few claudin-based cation channels, were small, their size was markedly increased when claudin-15 was expressed. Similarly, we found that increased expression of claudin-2, which, like claudin-15, forms a paracellular cation channel, was required for IL22-induced increases in enteroid volume treatment. We therefore conclude that, like zebrafish and MDCK cells, increases in luminal volume of IL22-treated enteroids were due to flux across paracellular cation channels rather than

epithelial proliferation. In contrast to enteroid enlargement, IL22 induced similar loss of wild-type, claudin-2 transgenic, and claudin-2 knockout enteroids. Thus, the effect of IL22 on stem cell loss is independent of claudin-2 expression.

Notch signaling guides the differentiation of progenitors into absorptive enterocytes in part by inhibiting secretory cell differentiation.^{37,39} Consistent with this, we found that IL22 prevented maturation of absorptive enterocytes, as indicated by reduced expression of mature enterocyte markers. Similar to our results, a recent study reported that IL33 decreased expression of both *Lgr5* and *Sucrase*, a marker of mature absorptive enterocytes, by inhibiting notch signaling.⁵³ Although we did not detect increased numbers of goblet cells, notch inhibition has been reported to cause goblet cell hyperplasia.^{39,47,54} Our result is most readily explained by ongoing wnt signaling, because notch inhibition in the presence of active wnt signaling is known to drive Paneth cell differentiation.^{35,40} Consistent with this idea, Zwarycz et al²¹ also found increased *Lyz* expression, but, interestingly, no change in Paneth cell numbers, in IL22-treated ileal enteroids. Thus, together with retained expression of some wnt target genes, transit-amplifying compartment expansion, and enhanced epithelial proliferation, the skewing toward Paneth cells suggests that wnt signaling is reduced, but not abolished, by IL22. Finally, our

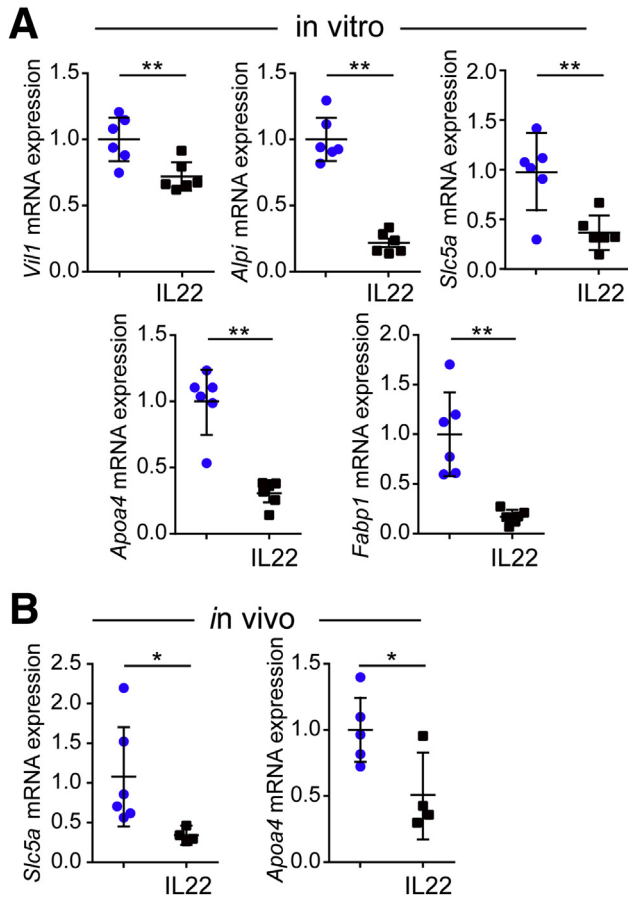


Figure 10. IL22 reduces enterocyte differentiation in vitro and in vivo. (A) Relative mRNA expression of mature enterocyte markers *Vil1*, *Alpi*, *Slc5a*, *ApoA4*, and *Fabp1* in jejunal enteroids cultured in ENR without (blue symbols) or with IL22 (black symbols) (5 ng/mL, PeproTech) for 3 days. $n = 6$ in the representative experiments shown. $*P < .05$; $**P < .01$. (B) Relative mRNA expression of mature enterocyte markers *Slc5a* and *ApoA4* in jejunal epithelial cells isolated from untreated and IL22-treated mice. $n = 4-7$ in the representative experiment shown. $*P < .05$.

data suggest that reduced endocrine cell differentiation may, in part, reflect activation of EGFR/MAPK signaling.

We conclude that IL22 promotes transit-amplifying cell proliferation but also reduces proliferative capacity and survival of *Lgr5*⁺ stem cells. This is mediated by alterations in signal transduction that also skew epithelial differentiation. In their studies of ileum and ileal enteroids, Zwarycz et al²¹ also found reduced wnt and notch signaling, but, surprisingly, identified somewhat different effects of IL22 on lineages. This is deserving of future study. Nevertheless, both studies demonstrate that, in the jejunum and ileum, IL22 links the immune system and epithelial function by multiple mechanisms, including expansion of the transit-amplifying compartment. These data further indicate that although IL22 may have potential as a therapeutic agent to promote mucosal healing, the timing of delivery relative to the disease process will likely require precise calibration.

Materials and Methods

Mice

C57BL/6 mice were purchased from the Jackson Laboratory or the Nanjing Biomedical Research Institute of Nanjing University. *Lgr5*-EGFP-IRES-CreER^{T2} mice⁵⁵ were purchased from the Jackson Laboratory. Claudin-2 knockout and claudin-2 transgenic mice were generated as described previously^{13,56} and maintained on a C57BL/6 background. Mice were maintained in SPF facilities. All experiments were conducted in accordance with the guidelines of the Animal Care and Use Committees of Soochow University, University of Chicago, Brigham and Women's Hospital, and Boston Children's Hospital.

Stem Cell (Enteroid) Culture

Mouse jejunal and ileal crypts were cultured as described to generate enteroids.⁵⁷ Specifically, ENR medium contained advanced Dulbecco modified Eagle medium/F12, 2 mmol/L Glutamax, 10 mmol/L HEPES, 100 U mL⁻¹ penicillin/streptomycin, 1 mmol/L N-acetyl cysteine, 1:50 B27 supplement, 1:100 N2 supplement, 50 ng mL⁻¹ EGF, 100 ng mL⁻¹ noggin, and 10% R-spondin-1 conditioned medium. Enteroids were grown in Growth Factor Reduced Matrigel (Corning Inc, Corning, NY; 356231), with the medium changed every 2-3 days. Enteroids were passaged weekly on the basis of daily microscopic observation and assessment of luminal debris accumulation. In designated experiments, culture media was supplemented with wnt- and R-spondin-conditioned media.³⁴

Interleukin 22 Treatment

Recombinant mouse IL22 was purchased from Pepro-Tech (201-22), GenScript (Z03350 and Z02197), and R&D Systems (582-ML-010 and 582-ML-010/CF), as indicated. IL22 was reconstituted in phosphate-buffered saline (PBS), as described by each manufacturer. IL22 was added to culture media 1 day after plating isolated crypts or 1 day after passage of established enteroid cultures. Results were similar with both procedures. When IL22-treated enteroids were propagated, they were passaged after 4 days because of increased enteroid size. In these experiments, enteroids that were not treated with IL22 were also passaged at 4 days. To inhibit JAK/STAT3 signaling, JAK Inhibitor I (Merck Millipore, Burlington, MA; 420099) or STAT3 inhibitor Stattic (MedChemExpress, Monmouth Junction, NJ; HY-13818) was added to ENR medium. Images were collected by using an inverted microscope (Olympus IX-73, Tokyo, Japan or Leica DMI-LED, Wetzlar, Germany). Enteroids were identified and counted manually. Cross-sectional area was determined by using ImageJ as described.²⁰

Cell and RNA Isolation for Quantitative Reverse Transcriptase Polymerase Chain Reaction

For analysis of in vitro gene expression, jejunal or ileal enteroids were broken by pipetting in PBS and collected by centrifugation at 900g for 5 minutes. For analysis of in vitro gene expression, jejunal epithelial cells were separated from

mesenchyme at 4°C by using Cell Recovery Solution (Corning; 354253), as described.⁵⁸ Total RNA was isolated from enteroids or isolated intestinal epithelial cells by using

the RNeasy Mini Kit (Qiagen, Hilden, Germany; 74106). RT-PCR was performed with an iScript cDNA Synthesis Kit (Bio-Rad, Hercules, CA; 1708891). Quantitative RT-PCR was performed on a CFX96 (Bio-Rad) system using specific primers (Table 1). Raw data were analyzed by Δ Ct using *Gapdh* for normalization. Expression changes were calculated by the $\Delta\Delta$ Ct method.

Enteroid Imaging and Staining

Enteroids were plated on chamber slides (Labtek, Grand Rapids, MI). To assess cell proliferation within enteroids, EdU incorporation was assessed by using the Click-iT EdU Imaging Kit (Invitrogen, Carlsbad, CA; C10339). Enteroids were incubated with EdU for 1 hour before fixation with 1% freshly-prepared paraformaldehyde (PFA). To detect cell death, enteroids were stained with 3 μ mol/L propidium iodide (Sigma, St Louis, MO; P4170) before fixation. Live cell imaging was used to detect caspase activation in cells incubated with CellEvent caspase-3/7 green detection reagent (Invitrogen; C10423).

For immunostaining, enteroids were grown on chamber slides, fixed with 1% PFA, washed with PBS, and blocked with 10% normal goat serum containing 50 mmol/L NH_4Cl for 30 minutes. Enteroids were incubated with antibodies against lysozyme (Abcam, Cambridge, MA; ab36362, 1:50 dilution), MUC2 (Santa Cruz Biotechnology, Dallas, TX; sc-15334, 1:200 dilution), or chromogranin A (Abcam; ab15160, 1:200 dilution) for 2 hours at room temperature. Afterwards, enteroids were washed with PBS containing 1% normal goat serum and incubated with Alexa Fluor 594 conjugated secondary antibodies (Invitrogen) and Hoechst (Invitrogen; H3570) for 1 hour at room temperature. Images were collected by confocal microscopy (Leica; TCS SP8X).

Flow Cytometry

Enteroids incubated with EdU, propidium iodide, or caspase-3/7 green detection reagent were collected by

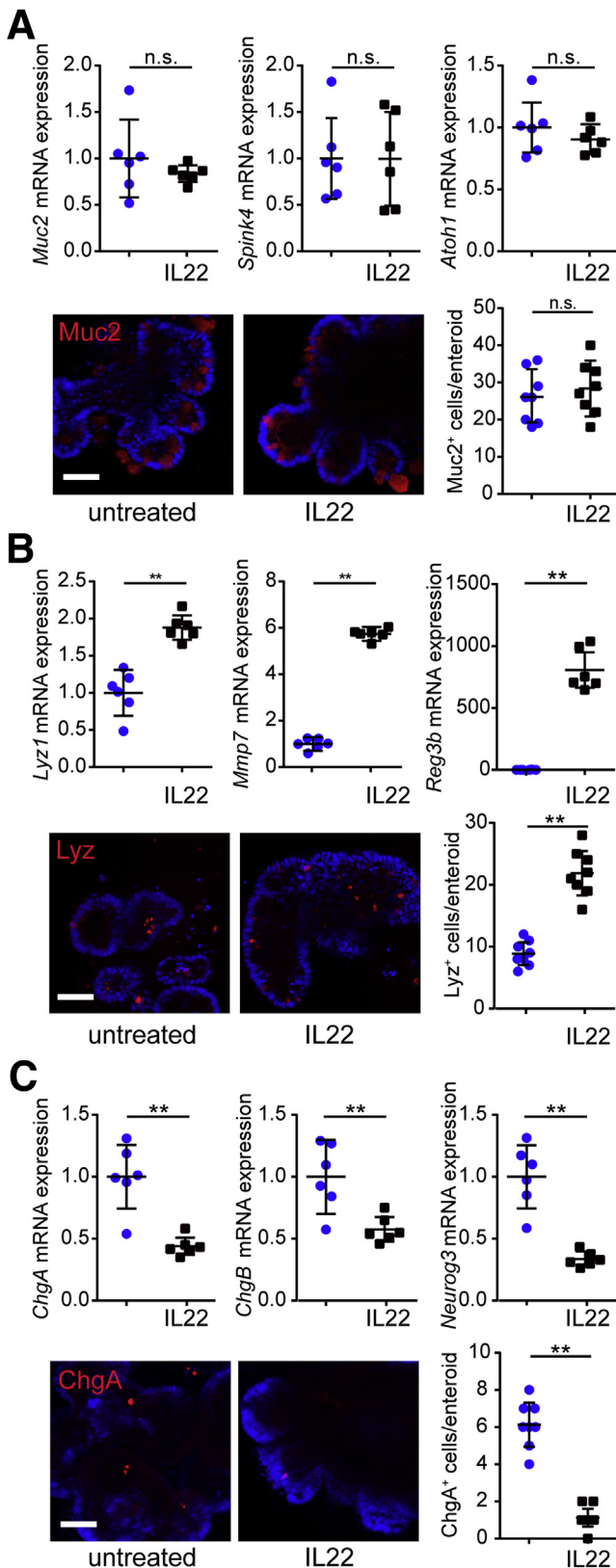


Figure 11. IL22 disrupts epithelial differentiation in vitro.

(A) Jejunal enteroids were cultured in ENR without (blue symbols) or with IL22 (black symbols) (5 ng/mL, PeproTech) for 3 days. mRNA expression of goblet cell markers *Muc2*, *Spink4*, and *Atoh1* was not affected ($n = 6$). Enteroids were immunostained for *Muc2* and nuclei (Hoechst). *Muc2*-positive cells per enteroid were counted ($n = 8$). Bar, 50 μ m. Representative data are shown. (B) Jejunal enteroids were cultured in ENR without (blue symbols) or with IL22 (black symbols) (5 ng/mL, PeproTech) for 3 days. mRNA expression of Paneth cell markers *Lyz1*, *Mmp7*, and *Reg3b* was increased after IL22 treatment ($n = 6$). Enteroids were immunostained for lysosome (Lyz) and nuclei (Hoechst). Lysosome-positive cells per enteroid were counted ($n = 8$). Bar, 50 μ m. Representative data are shown. $**P < .01$. (C) Jejunal enteroids were cultured in ENR without or with IL22 for 3 days. mRNA expression of endocrine cell markers *ChgA*, *ChgB*, and *Neurog3* was decreased after IL22 treatment ($n = 6$). Enteroids were immunostained for chromogranin A (*ChgA*) and nuclei (Hoechst). Chromogranin A-positive cells per enteroid were counted ($n = 8$). Bar, 50 μ m. Representative data are shown. $**P < .01$.

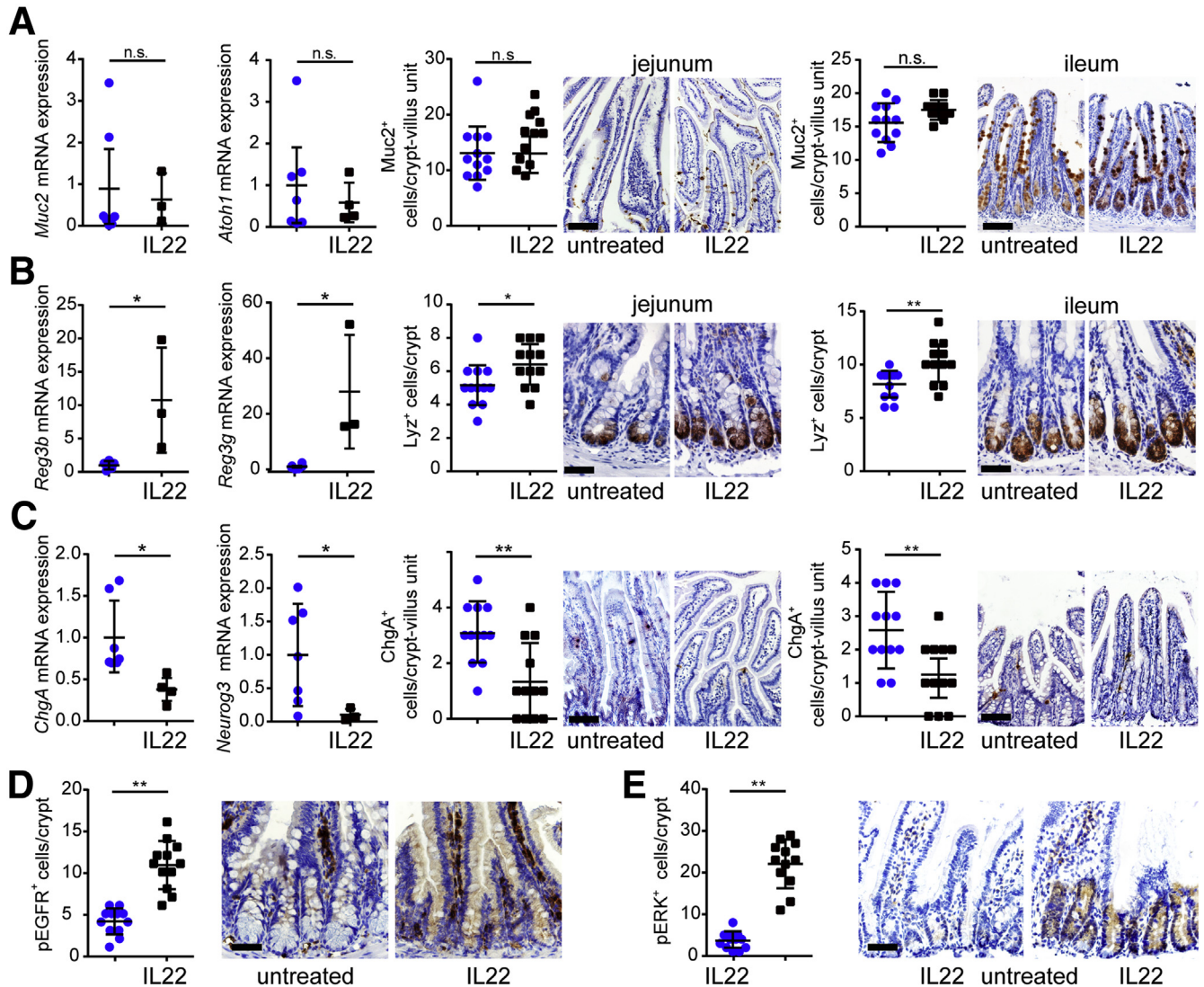


Figure 12. IL22 disrupts epithelial differentiation in vivo. (A) Jejunal epithelial cells were isolated from untreated or IL22-treated mice. mRNA expression of goblet cell markers *Muc2* and *Atoh1* was not affected by IL22 treatment ($n = 4-7$). Jejunal and ileal tissues were immunostained for *Muc2*, and positive cells per crypt were counted ($n = 12$). Bar, 100 μm . Representative data are shown. (B) Jejunal epithelial cells were isolated from untreated or IL22-treated mice. mRNA expression of Paneth cell markers *Reg3b* and *Reg3g* was increased by IL22 treatment ($n = 3-7$). Jejunal and ileal tissues were immunostained for lysosome (*Lyz*), and positive cells per crypt were counted ($n = 12$). Bar, 50 μm . Representative data are shown. * $P < .05$; ** $P < .01$. (C) Jejunal epithelial cells were isolated from untreated or IL22-treated mice. mRNA expression of endocrine cell markers *ChgA* and *Neurog3* was reduced by IL22 treatment ($n = 4-7$). Jejunal and ileal tissues were immunostained for chromogranin A (*ChgA*), and positive cells per crypt were counted ($n = 12$). Bar, 100 μm . Representative data are shown. * $P < .05$; ** $P < .01$. (D) Jejunal tissue from untreated or IL22-treated mice was immunostained for phosphorylated EGFR. Numbers of positive cells per crypt were counted ($n = 12$). Bar, 50 μm . Representative data are shown. ** $P < .01$. (E) Jejunal tissue from untreated or IL22-treated mice were immunostained for phosphorylated ERK (pERK), and positive cells per crypt were counted ($n = 12$). Bar, 50 μm . Representative data are shown. ** $P < .01$.

centrifugation at 900g for 5 minutes, washed once with PBS, and incubated for 10 minutes with TrypLE (Thermo Fisher, Waltham, MA; 12605036) at 37°C. For EdU detection, cells were fixed and labeled using Click-iT (Invitrogen). Enteroids were separated into single cells by vigorous pipetting. Single cells were washed once with PBS, resuspended, and passed through a 70 μm filter (BD Falcon, Franklin Lakes, NJ). To analyze *Lgr5*-EGFP⁺ cells, enteroids were isolated from *Lgr5*-EGFP-IRES-CreER^{T2} mice and cultured in ENR without

or with IL22. Flow cytometry was performed by using an Attune NxT acoustic focusing cytometer (Invitrogen). FlowJo software was used for data analysis.

Histology, Immunohistochemistry, and Immunofluorescence Staining

Formalin-fixed tissue sections were embedded in paraffin by standard methods. Sections (5 μm) were

Table 1. Quantitative RT-PCR Primer Sequences

Gene	Forward primer (5'–3')	Reverse primer (5'–3')
<i>Alpi</i>	GGCCATCTAGGACCGGAGA	TGTCCACGTTGTATGTCTTGG
<i>Apoa4</i>	CAACAGGCTGAAGGCTACGAT	CGATTTTTGCGGAGACCTTGG
<i>Ascl2</i>	CTACTCGTCGGAGGAAAG	ACTAGACAGCATGGGTAAG
<i>Atoh1</i>	GAGTGGGCTGAGGTAAAAGAGT	GGTCGGTGCTATCCAGGAG
<i>Axin2</i>	GGACTGGGGAGCCTAAAGGT	AAGGAGGGACTCCATCTACGC
<i>Bmi1</i>	ATCCCCACTTAATGTGTGTCTCT	CTTGCTGGTCTCCAAGTAACG
<i>Cd3</i>	ATGCGGTGGAACACTTTCTGG	GCACGTCAACTCTACACTGGT
<i>Cd44</i>	CACCATTGCCTCAACTGTGC	TTGTGGGCTCCTGAGTCTGA
<i>ChgA</i>	CCAAGGTGATGAAGTGCCTC	GGTGTGCGCAGGATAGAGAGGA
<i>ChgB</i>	GCTCAGCTCCAGTGGATAACA	CAGGGGTGATCGTTGGAACAC
<i>Cldn2</i>	GGCTGTTAGGCACATCCAT	TGGCACCAACATAGGAACTC
<i>Cmyc</i>	TTCATCTGCGATCCTGACGAC	CACTGAGGGGTCAATGCACCTC
<i>Dkk1</i>	TGCATGAGGCACGCTATGTG	GCGGCGTTGTGGTCATTAC
<i>Dkk2</i>	ACCCGCTGCAATAATGGAATC	ATGGTTGCGATCTCTATGCCG
<i>Dll1</i>	GCAGGACCTTCTTCGCGTAT	AAGGGGAATCGGATGGGGTT
<i>Dll4</i>	TTCCAGGCAACCTTCTCCGA	ACTGCCGCTATTCTTGTCCC
<i>F4/80</i>	TGACTCACCTTGTGGTCTCTAA	CTTCCCAGAATCCAGTCTTTCC
<i>Fabp1</i>	ATGAACTTCTCCGGCAAGTACC	CTGACACCCCTTGATGTCC
<i>Fzd7</i>	CGGGGCCTCAAGGAGAGAA	GTCCCCTAAACCAGCCAG
<i>Gapdh</i>	AGGTCGGTGTGAACGGATTTG	GGGGTCGTTGATGGCAACA
<i>Hes1</i>	TCAACACGACACCCGACAAAC	ATGCCGGGAGCTATCTTTCTT
<i>Hopx</i>	ACCACGCTGTGCCTCATCGC	TTCTGACCGCCGCACTCTG
<i>Jagged1</i>	CCTCGGGTCAGTTTGAGCTG	CCTTGAGGCACACTTTGAAGTA
<i>Ki67</i>	ATCATTGACCGCTCCTTTAGGT	GCTCGCCTTGATGGTTCCT
<i>Lgr5</i>	CCTACTCGAAGACTTACCCAGT	GCATTGGGGTGAATGATAGCA
<i>Lrig1</i>	TTGAGGACTTGACGAATCTGC	CTTGTGTGCTGCAAAAAGAGAG
<i>Lrp5</i>	AAGGGTGCTGTGACTGGAC	AGAAGAGAACCTTACGGGACG
<i>Lrp6</i>	TTGTTGCTTTATGCAACAGACG	GTTCGTTAATGGCTTCTTCGC
<i>Lyz1</i>	GGAATGGATGGCTACCGTGG	CATGCCACCCATGCTCGAAT
<i>Mmp7</i>	CTGCCACTGTCCCAGGAAG	GGGAGAGTTTTCCAGTCATGG
<i>Mpo</i>	AGTTGTGCTGAGCTGTATGGA	CGGCTGCTTGAAGTAAACAGG
<i>Muc2</i>	ATGCCACCTCCTCAAAGAC	GTAGTTTCCGTTGGAACAGTGAA
<i>Neurog 3</i>	CCAAGAGCGAGTTGGCACT	CGGGCCATAGAAGCTGTGG
<i>Notch1</i>	GATGGCCTCAATGGGTACAAG	TCGTTGTTGTTGATGTCACAGT
<i>Olfm4</i>	GCCACTTCCAATTTAC	GAGCCTCTTCTCATAAC
<i>Pcna</i>	TTTGAGGCACGCCTGATCC	GGAGACGTGAGACGAGTCCAT
<i>Prom1</i>	CTCCCATCAGTGGATAGAGAAT	ATACCCCTTTTACGAGGCT
<i>Prss32</i>	GCCTGCCATCCTATTTACCTTC	AGTCCAAGTCAATGCTCCTCC
<i>Reg3b</i>	ACTCCCTGAAGAATATACCCTCC	CGCTATTGAGCACAGATACGAG
<i>Reg3g</i>	ATGCTTCCCCGTATAACCATCA	GGCCATATCTGCATCATAACGAG
<i>Rnf43</i>	TCCGAAAGATCAGCAGAACAGA	GGACTGCATTAGCTTCCCTTC
<i>Slc5a</i>	ATGCGGCTGACATCTCAGTC	ACCAAGGCGTTCCATTCAAAG
<i>Sox9</i>	GAGCCGGATCTGAAGAGGGA	GCTTGACGTGTGGCTTGTTC
<i>Tert</i>	TCTACCGCACTTTGGTTGCC	CAGCACGTTTCTCTCGTTGC
<i>Vil1</i>	TCAAAGGCTCTCTCAACATCAC	AGCAGTACCATCGAAGAAGC
<i>Wif1</i>	GATCCAAGTGTCAATGTCCCTT	ACACGGGAAACCAACTTGAAC
<i>Wnt3</i>	TGGAAGTGTACCACCATAGATGAC	ACACCAGCCGAGGCGATG
<i>Zpf652</i>	GGAGCTGGTTGAACCTGTG	AGGGCTTCCAGACTCCCTTTT

deparaffinized in xylene and rehydrated with graded ethanols, and antigen retrieval was performed by boiling in citrate buffer (pH 6) in a vegetable steamer for 20 minutes. Slides were then treated with 3% hydrogen peroxide for 5 minutes and washed with PBS before addition of primary antibodies against GFP (Sigma; G1544, 1:1000 dilution), Ki-67 (Cell Signaling Technology, Danvers, MA; 12202, 1:500 dilution), OLFM4 (Cell Signaling Technology; 39141, 1:400 dilution), Phospho-p44/42 MAPK (Erk1/2) (Thr202/Tyr204) (Cell Signaling Technology; 9101, 1:800 dilution), lysozyme (Abcam; ab108508, 1:4000 dilution), MUC2 (Santa Cruz Biotechnology; sc-15334), and chromogranin A (Abcam; ab15160), or for 18 hours at 4°C. Afterwards, the slides were washed with PBS, incubated with horseradish peroxidase-conjugated secondary antibodies for 1 hour, developed by using the DAB Peroxidase (HRP) Substrate Kit (Vector Laboratories, Burlingame, CA), and counterstained with hematoxylin.

Frozen sections of jejunum were fixed with 1% PFA, washed with PBS, and blocked with 10% normal goat serum containing 50 mmol/L NH₄Cl for 30 minutes. Tissues were incubated with antibodies against CD3 (Abcam; ab16669, 1:100 dilution), F4/80 (eFluor 570 conjugated; eBiosciences, San Diego, CA; 41-4801-80, 1:200 dilution), or myeloperoxidase (Abcam; ab9535, 1:200 dilution) for 2 hours at room temperature. Tissues were then washed with PBS containing 1% normal goat serum and incubated with secondary antibodies and Hoechst (Life Technologies, Carlsbad, CA; H3570) for 1 hour at room temperature. Images were collected using confocal microscopy (Leica; TCS SP8X).

For morphometry, at least 2 fields containing well-oriented crypts-villus units were assessed for each mouse. The average number of positive cells in each field is shown as a single point in the graphs.

In Vivo Interleukin 22 Administration

C57BL/6 or Lgr5-EGFP-IRES-CreER^{T2} mice were injected intraperitoneally with IL22 (dissolved in saline 1 µg/mL, 1 µg/day) or vehicle for 7 consecutive days. Intestinal tissues were collected on day 8 and either used for isolation of crypts or epithelial cells, as above, or fixed in formalin for immunohistochemical analysis.

Statistical Analysis

All data are representative of at least 3 independent experiments. Values are mean ± standard deviation. Two-tailed Student *t* test was used to compare 2 groups. One-way analysis of variance was used to compare 3 or more groups. Specific numbers of enteroids or mice are noted in each figure legend. **P* < .05 and ***P* < .01 were considered significant.

References

1. Sato T, van Es JH, Snippert HJ, Stange DE, Vries RG, van den Born M, Barker N, Shroyer NF, van de Wetering M, Clevers H. Paneth cells constitute the niche for Lgr5 stem cells in intestinal crypts. *Nature* 2011; 469:415–418.
2. Clevers H, Loh KM, Nusse R. Stem cell signaling: an integral program for tissue renewal and regeneration—Wnt signaling and stem cell control. *Science* 2014;346:1248012.
3. Miyoshi H, Ajima R, Luo CT, Yamaguchi TP, Stappenbeck TS. Wnt5a potentiates TGF-beta signaling to promote colonic crypt regeneration after tissue injury. *Science* 2012;338:108–113.
4. Ikeuchi H, Kuroiwa T, Hiramatsu N, Kaneko Y, Hiromura K, Ueki K, Nojima Y. Expression of interleukin-22 in rheumatoid arthritis: potential role as a proinflammatory cytokine. *Arthritis Rheum* 2005;52: 1037–1046.
5. Wolk K, Haugen HS, Xu W, Witte E, Waggie K, Anderson M, Vom Baur E, Witte K, Warszawska K, Philipp S, Johnson-Leger C, Volk HD, Sterry W, Sabat R. IL-22 and IL-20 are key mediators of the epidermal alterations in psoriasis while IL-17 and IFN-gamma are not. *J Mol Med (Berl)* 2009;87:523–536.
6. Justa S, Zhou X, Sarkar S. Endogenous IL-22 plays a dual role in arthritis: regulation of established arthritis via ifn-gamma responses. *PLoS One* 2014;9:e93279.
7. Leipe J, Schramm MA, Grunke M, Baeuerle M, Dechant C, Nigg AP, Witt MN, Vielhauer V, Reindl CS, Schulze-Koops H, Skapenko A. Interleukin 22 serum levels are associated with radiographic progression in rheumatoid arthritis. *Ann Rheum Dis* 2011; 70:1453–1457.
8. Pantelyushin S, Haak S, Ingold B, Kulig P, Heppner FL, Navarini AA, Becher B. Rorγ⁺ innate lymphocytes and gammadelta T cells initiate psoriasiform plaque formation in mice. *J Clin Invest* 2012;122:2252–2256.
9. Munoz M, Heimesaat MM, Danker K, Struck D, Lohmann U, Plickert R, Bereswill S, Fischer A, Dunay IR, Wolk K, Loddenkemper C, Krell HW, Libert C, Lund LR, Frey O, Holscher C, Iwakura Y, Ghilardi N, Ouyang W, Kamradt T, Sabat R, Liesenfeld O. Interleukin (IL)-23 mediates toxoplasma gondii-induced immunopathology in the gut via matrixmetalloproteinase-2 and IL-22 but independent of IL-17. *J Exp Med* 2009; 206:3047–3059.
10. Kamanaka M, Huber S, Zenewicz LA, Gagliani N, Rathinam C, O'Connor W Jr, Wan YY, Nakae S, Iwakura Y, Hao L, Flavell RA. Memory/effector (CD45RB^{lo}) CD4 T cells are controlled directly by IL-10 and cause IL-22-dependent intestinal pathology. *J Exp Med* 2011;208:1027–1040.
11. Zhao K, Zhao D, Huang D, Yin L, Chen C, Pan B, Wu Q, Li Z, Yao Y, Shen E, Zeng L, Xu K. Interleukin-22 aggravates murine acute graft-versus-host disease by expanding effector T cell and reducing regulatory T cell. *J Interferon Cytokine Res* 2014;34:707–715.
12. Zhao J, Zhang Z, Luan Y, Zou Z, Sun Y, Li Y, Jin L, Zhou C, Fu J, Gao B, Fu Y, Wang FS. Pathological functions of interleukin-22 in chronic liver inflammation and fibrosis with hepatitis B virus infection by promoting

- T helper 17 cell recruitment. *Hepatology* 2014; 59:1331–1342.
13. Tsai PY, Zhang B, He WQ, Zha JM, Odenwald MA, Singh G, Tamura A, Shen L, Sailer A, Yeruva S, Kuo WT, Fu YX, Tsukita S, Turner JR. IL-22 upregulates epithelial claudin-2 to drive diarrhea and enteric pathogen clearance. *Cell Host Microbe* 2017; 21:671–681 e4.
 14. Tumino M, Serafin V, Accordi B, Spadini S, Forest C, Cortese G, Lissandron V, Marzollo A, Basso G, Messina C. Interleukin-22 in the diagnosis of active chronic graft-versus-host disease in paediatric patients. *Br J Haematol* 2015;168:142–145.
 15. Zenewicz LA, Yancopoulos GD, Valenzuela DM, Murphy AJ, Stevens S, Flavell RA. Innate and adaptive interleukin-22 protects mice from inflammatory bowel disease. *Immunity* 2008;29:947–957.
 16. Sugimoto K, Ogawa A. IL-22 ameliorates intestinal inflammation in a mouse model of ulcerative colitis. *J Clin Invest* 2008;118:534–544.
 17. Giacomini PR, Moy RH, Noti M, Osborne LC, Siracusa MC, Alenghat T, Liu B, McCorkell KA, Troy AE, Rak GD, Hu Y, May MJ, Ma HL, Fouser LA, Sonnenberg GF, Artis D. Epithelial-intrinsic IKK α expression regulates group 3 innate lymphoid cell responses and antibacterial immunity. *J Exp Med* 2015; 212:1513–1528.
 18. Hainzl E, Stockinger S, Rauch I, Heider S, Berry D, Lassnig C, Schwab C, Rosebrock F, Milinovich G, Schleder M, Wagner M, Schleper C, Loy A, Urich T, Kenner L, Han X, Decker T, Strobl B, Muller M. Intestinal epithelial cell tyrosine kinase 2 transduces IL-22 signals to protect from acute colitis. *J Immunol* 2015; 195:5011–5024.
 19. Aparicio-Domingo P, Romera-Hernandez M, Karrich JJ, Cornelissen F, Papazian N, Lindenbergh-Kortleve DJ, Butler JA, Boon L, Coles MC, Samsom JN, Cupedo T. Type 3 innate lymphoid cells maintain intestinal epithelial stem cells after tissue damage. *J Exp Med* 2015; 212:1783–1791.
 20. Lindemans CA, Calafiore M, Mertelsmann AM, O'Connor MH, Dudakov JA, Jenq RR, Velardi E, Young LF, Smith OM, Lawrence G, Ivanov JA, Fu YY, Takashima S, Hua G, Martin ML, O'Rourke KP, Lo YH, Mokry M, Romera-Hernandez M, Cupedo T, Dow LE, Nieuwenhuis EE, Shroyer NF, Liu C, Kolesnick R, van den Brink MR, Hanash AM. Interleukin-22 promotes intestinal-stem-cell-mediated epithelial regeneration. *Nature* 2015;528:560–564.
 21. Zwarycz B, Gracz AD, Rivera KR, Williamson IA, Samsa LA, Starmer J, Daniele MA, Salter-Cid L, Zhao Q, Magness ST. IL22 inhibits epithelial stem cell expansion in an ileal organoid model. *Cell Mol Gastroenterol Hepatol* 2019;7:1–17.
 22. Rosenthal R, Milatz S, Krug SM, Oelrich B, Schulzke JD, Amasheh S, Gunzel D, Fromm M. Claudin-2, a component of the tight junction, forms a paracellular water channel. *J Cell Sci* 2010;123:1913–1921.
 23. Weber CR, Liang GH, Wang Y, Das S, Shen L, Yu AS, Nelson DJ, Turner JR. Claudin-2-dependent paracellular channels are dynamically gated. *Elife* 2015;4:e09906.
 24. Yu AS, Cheng MH, Angelow S, Gunzel D, Kanzawa SA, Schneeberger EE, Fromm M, Coalson RD. Molecular basis for cation selectivity in claudin-2-based paracellular pores: identification of an electrostatic interaction site. *J Gen Physiol* 2009;133:111–127.
 25. Ahmad R, Chaturvedi R, Olivares-Villagomez D, Habib T, Asim M, Shivesh P, Polk DB, Wilson KT, Washington MK, Van Kaer L, Dhawan P, Singh AB. Targeted claudin-2 expression renders resistance to epithelial injury, induces immune suppression, and protects from colitis. *Mucosal Immunol* 2014;7:1340–1353.
 26. Dhawan P, Ahmad R, Chaturvedi R, Smith JJ, Midha R, Mittal MK, Krishnan M, Chen X, Eschrich S, Yeatman TJ, Harris RC, Washington MK, Wilson KT, Beauchamp RD, Singh AB. Claudin-2 expression increases tumorigenicity of colon cancer cells: role of epidermal growth factor receptor activation. *Oncogene* 2011;30:3234–3247.
 27. Schuijers J, Junker JP, Mokry M, Hatzis P, Koo BK, Sasselli V, van der Flier LG, Cuppen E, van Oudenaarden A, Clevers H. *Ascl2* acts as an R-spondin/Wnt-responsive switch to control stemness in intestinal crypts. *Cell Stem Cell* 2015;16:158–170.
 28. Haber AL, Biton M, Rogel N, Herbst RH, Shekhar K, Smillie C, Burgin G, Delorey TM, Howitt MR, Katz Y, Tirosh I, Beyaz S, Dionne D, Zhang M, Raychowdhury R, Garrett WS, Rozenblatt-Rosen O, Shi HN, Yilmaz O, Xavier RJ, Regev A. A single-cell survey of the small intestinal epithelium. *Nature* 2017; 551:333–339.
 29. Clevers H. The intestinal crypt, a prototype stem cell compartment. *Cell* 2013;154:274–284.
 30. Roche KC, Gracz AD, Liu XF, Newton V, Akiyama H, Magness ST. Sox9 maintains reserve stem cells and preserves radioresistance in mouse small intestine. *Gastroenterology* 2015;149:1553–1563 e10.
 31. Wong VW, Stange DE, Page ME, Buczaccki S, Wabik A, Itami S, van de Wetering M, Poulsom R, Wright NA, Trotter MW, Watt FM, Winton DJ, Clevers H, Jensen KB. *Lrig1* controls intestinal stem-cell homeostasis by negative regulation of *erbb* signalling. *Nat Cell Biol* 2012; 14:401–408.
 32. Powell AE, Wang Y, Li Y, Poulin EJ, Means AL, Washington MK, Higginbotham JN, Juchheim A, Prasad N, Levy SE, Guo Y, Shyr Y, Aronow BJ, Haigis KM, Franklin JL, Coffey RJ. The pan-*erbb* negative regulator *Lrig1* is an intestinal stem cell marker that functions as a tumor suppressor. *Cell* 2012; 149:146–158.
 33. Sato T, Clevers H. Growing self-organizing mini-guts from a single intestinal stem cell: mechanism and applications. *Science* 2013;340:1190–1194.
 34. Miyoshi H, Stappenbeck TS. In vitro expansion and genetic modification of gastrointestinal stem cells in spheroid culture. *Nat Protoc* 2013;8:2471–2482.

35. Yin X, Farin HF, van Es JH, Clevers H, Langer R, Karp JM. Niche-independent high-purity cultures of Lgr5⁺ intestinal stem cells and their progeny. *Nat Methods* 2014;11:106–112.
36. Tian H, Biehs B, Chiu C, Siebel CW, Wu Y, Costa M, de Sauvage FJ, Klein OD. Opposing activities of notch and wnt signaling regulate intestinal stem cells and gut homeostasis. *Cell Rep* 2015;11:33–42.
37. Demitrack ES, Samuelson LC. Notch regulation of gastrointestinal stem cells. *J Physiol* 2016; 594:4791–4803.
38. Noah TK, Shroyer NF. Notch in the intestine: regulation of homeostasis and pathogenesis. *Annu Rev Physiol* 2013;75:263–288.
39. VanDussen KL, Carulli AJ, Keeley TM, Patel SR, Puthoff BJ, Magness ST, Tran IT, Maillard I, Siebel C, Kolterud A, Grosse AS, Gumucio DL, Ernst SA, Tsai YH, Dempsey PJ, Samuelson LC. Notch signaling modulates proliferation and differentiation of intestinal crypt base columnar stem cells. *Development* 2012;139: 488–497.
40. van Es JH, Sato T, van de Wetering M, Lyubimova A, Nee AN, Gregorieff A, Sasaki N, Zeinstra L, van den Born M, Korving J, Martens AC, Barker N, van Oudenaarden A, Clevers H. Dll1⁺ secretory progenitor cells revert to stem cells upon crypt damage. *Nat Cell Biol* 2012;14:1099–1104.
41. Basak O, Beumer J, Wiebrands K, Seno H, van Oudenaarden A, Clevers H. Induced quiescence of Lgr5⁺ stem cells in intestinal organoids enables differentiation of hormone-producing enteroendocrine cells. *Cell Stem Cell* 2017;20:177–190 e4.
42. Brand S, Beigel F, Olszak T, Zitzmann K, Eichhorst ST, Otte JM, Diepolder H, Marquardt A, Jagla W, Popp A, Leclair S, Herrmann K, Seiderer J, Ochsenkuhn T, Goke B, Auernhammer CJ, Dambacher J. IL-22 is increased in active Crohn's disease and promotes proinflammatory gene expression and intestinal epithelial cell migration. *Am J Physiol Gastrointest Liver Physiol* 2006;290:G827–G838.
43. Andoh A, Zhang Z, Inatomi O, Fujino S, Deguchi Y, Araki Y, Tsujikawa T, Kitoh K, Kim-Mitsuyama S, Takayanagi A, Shimizu N, Fujiyama Y. Interleukin-22, a member of the IL-10 subfamily, induces inflammatory responses in colonic subepithelial myofibroblasts. *Gastroenterology* 2005;129:969–984.
44. Couturier M, Lamarthee B, Arbez J, Renauld JC, Bossard C, Malard F, Bonnefoy F, Mohty M, Perruche S, Tiberghien P, Saas P, Gaugler B. IL-22 deficiency in donor T cells attenuates murine acute graft-versus-host disease mortality while sparing the graft-versus-leukemia effect. *Leukemia* 2013;27:1527–1537.
45. Snippert HJ, van Es JH, van den Born M, Begthel H, Stange DE, Barker N, Clevers H. Prominin-1/CD133 marks stem cells and early progenitors in mouse small intestine. *Gastroenterology* 2009;136: 2187–2194 e1.
46. Snippert HJ, van der Flier LG, Sato T, van Es JH, van den Born M, Kroon-Veenboer C, Barker N, Klein AM, van Rhee J, Simons BD, Clevers H. Intestinal crypt homeostasis results from neutral competition between symmetrically dividing Lgr5 stem cells. *Cell* 2010; 143:134–144.
47. Pellegrinet L, Rodilla V, Liu Z, Chen S, Koch U, Espinosa L, Kaestner KH, Kopan R, Lewis J, Radtke F. Dll1- and Dll4-mediated notch signaling are required for homeostasis of intestinal stem cells. *Gastroenterology* 2011;140:1230–1240 e1–e7.
48. Buczaccki SJ, Zecchini HI, Nicholson AM, Russell R, Vermeulen L, Kemp R, Winton DJ. Intestinal label-retaining cells are secretory precursors expressing Lgr5. *Nature* 2013;495:65–69.
49. Wang Y, Mumm JB, Herbst R, Kolbeck R, Wang Y. IL-22 increases permeability of intestinal epithelial tight junctions by enhancing claudin-2 expression. *J Immunol* 2017;199:3316–3325.
50. Rosenthal R, Gunzel D, Krug SM, Schulzke JD, Fromm M, Yu AS. Claudin-2-mediated cation and water transport share a common pore. *Acta Physiol (Oxf)* 2017; 219:521–536.
51. Amasheh S, Meiri N, Gitter AH, Schoneberg T, Mankertz J, Schulzke JD, Fromm M. Claudin-2 expression induces cation-selective channels in tight junctions of epithelial cells. *J Cell Sci* 2002; 115:4969–4976.
52. Bagnat M, Cheung ID, Mostov KE, Stainier DY. Genetic control of single lumen formation in the zebrafish gut. *Nat Cell Biol* 2007;9:954–960.
53. Mahapatro M, Foersch S, Hefele M, He GW, Giner-Ventura E, McHedlidze T, Kindermann M, Vetrano S, Danese S, Gunther C, Neurath MF, Wirtz S, Becker C. Programming of intestinal epithelial differentiation by IL-33 derived from pericryptal fibroblasts in response to systemic infection. *Cell Rep* 2016;15:1743–1756.
54. Durand A, Donahue B, Peignon G, Letourneur F, Cagnard N, Slomianny C, Perret C, Shroyer NF, Romagnolo B. Functional intestinal stem cells after paneth cell ablation induced by the loss of transcription factor Math1 (Atoh1). *Proc Natl Acad Sci U S A* 2012; 109:8965–8970.
55. Barker N, van Es JH, Kuipers J, Kujala P, van den Born M, Cozijnsen M, Haegebarth A, Korving J, Begthel H, Peters PJ, Clevers H. Identification of stem cells in small intestine and colon by marker gene Lgr5. *Nature* 2007;449:1003–1007.
56. Tamura A, Hayashi H, Imasato M, Yamazaki Y, Hagiwara A, Wada M, Noda T, Watanabe M, Suzuki Y, Tsukita S. Loss of claudin-15, but not claudin-2, causes Na⁺ deficiency and glucose malabsorption in mouse small intestine. *Gastroenterology* 2011;140:913–923.
57. Sato T, Vries RG, Snippert HJ, van de Wetering M, Barker N, Stange DE, van Es JH, Abo A, Kujala P, Peters PJ, Clevers H. Single Lgr5 stem cells build crypt-villus structures in vitro without a mesenchymal niche. *Nature* 2009;459:262–265.
58. Nik AM, Carlsson P. Separation of intact intestinal epithelium from mesenchyme. *Biotechniques* 2013; 55:42–44.

Received March 13, 2018. Accepted September 6, 2018.

Correspondence

Address correspondence to: Jerrold R. Turner, PhD, MD, Department of Pathology, Brigham and Women's Hospital and Harvard Medical School, Boston, Massachusetts 02115. e-mail: jrtturner@bwh.harvard.edu; fax: (773) 834-5251; and Wei-Qi He, PhD, Cambridge-Suda (CAM-SU) Genome Resource Center, Soochow University, Suzhou, China. e-mail: whe@suda.edu.cn.

Author contributions

J.Z., J.R.T., and W.H. designed experiments, analyzed data, and prepared this manuscript. J.P., X.Z., K.C., and M.T. analyzed data and discussed the results. J.Z., H.L., Q.L., Z.J., P.T., W.K., N.D., J.W., S.X., Y.W., M.A.O., J.R.T., and W.H. performed experiments. A.T. and S.T. provided critical reagents. All authors reviewed and approved the submitted manuscript.

Conflicts of interest

The authors disclose no conflicts.

Funding

Funded by National Natural Science Foundation of China (81470804 and 31401229 to W.H.; 81200620 to J.Z.; 81570125 to J.P.), the Natural Science Foundation of Jiangsu Province (BK20140319 to W.H.), The Research Innovation Program for College Graduates of Jiangsu Province (KYLX16-0116 to H.L.; KYCX17-2033 to Z.J.), Advanced Research Projects of Soochow University (SDY2015B06 to J.Z.), Crohn's & Colitis Foundation Research Fellowship Award (310801 to W.H.), the National Institute of Diabetes and Digestive and Kidney Diseases (R01DK061931 and R01DK068271 to J.R.T. and F30DK103511 to M.A.O.), and the Harvard Digestive Disease Center (P30DK034854). This work was also supported by International Joint Research Center for Genomic Resources (2017B01012).